Modeling Thomson-Scattering Measurements of Multibeam Two-Plasmon Decay

TPD-driven Thomson-scattering spectrum

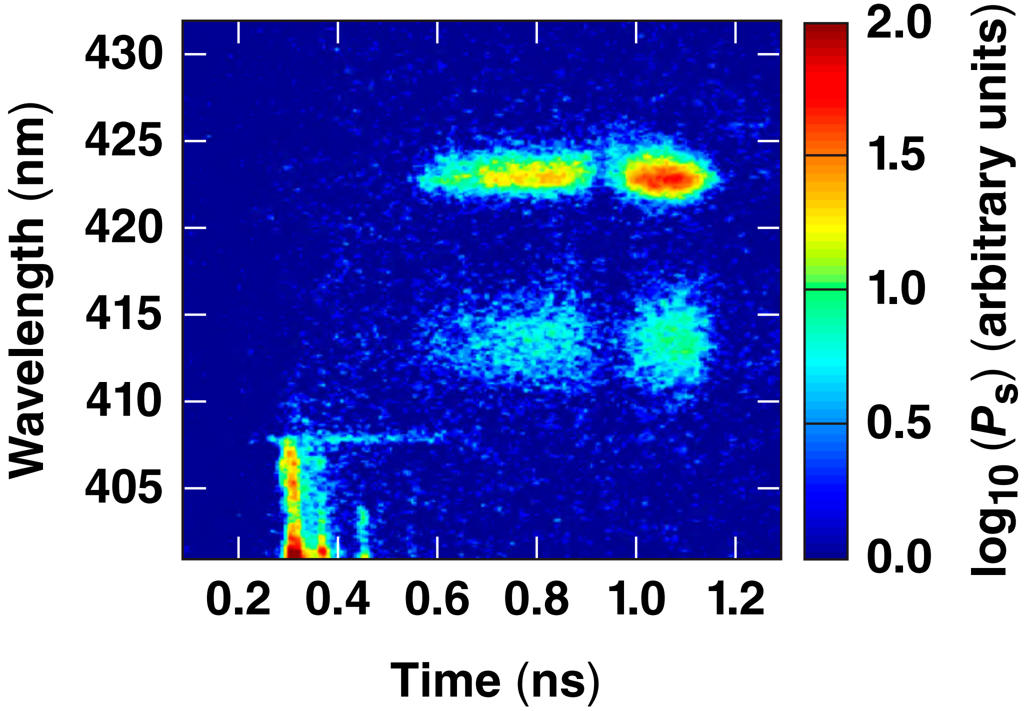

Spectral lineouts (1.1 ns)

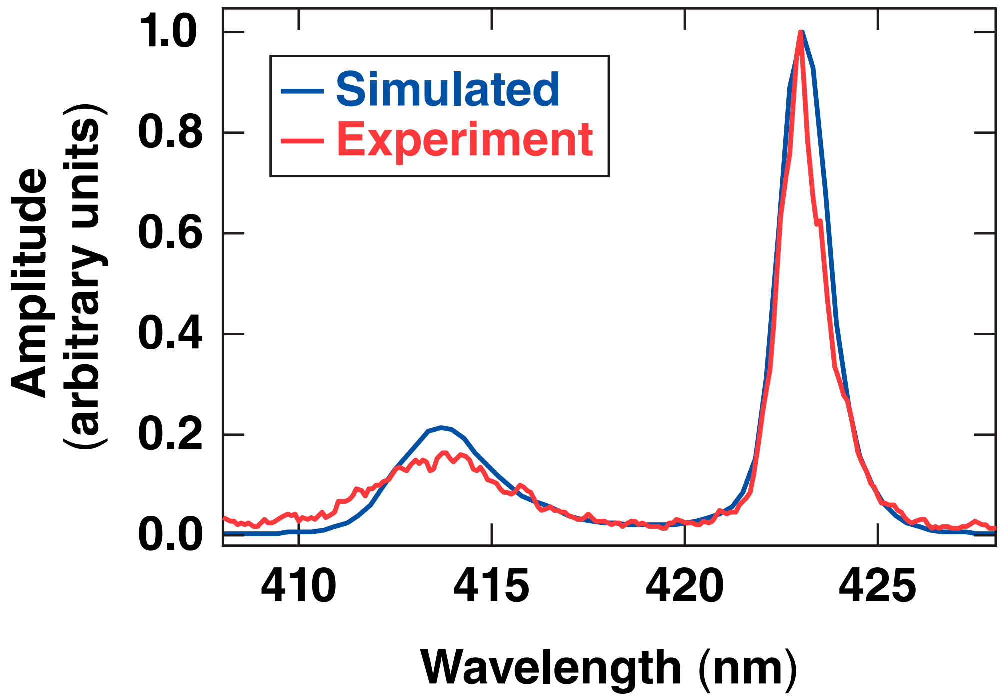

R. K. Follett
University of Rochester
Laboratory for Laser Energetics

45th Annual Anomalous Absorption Conference
Ventura, CA
14–19 June 2015

Summary

Three-dimensional two-plasmon–decay (TPD) simulations were used to reproduce experimental observations

- *LPSE* (laser-plasma simulation environment) was used to simulate Thomson-scattering (TS) from TPD-driven waves
- The Thomson-scattering spectra shows two large-amplitude peaks corresponding to TPD-driven waves
- A hybrid-particle model was used to calculate the hot-electron distribution
- The simulations reproduce the observed scaling of hot-electron temperature and fraction

Collaborators

J. Shaw, D. H. Edgell, R. J. Henchen, S. X. Hu, J. Katz, D. T. Michel,
J. F. Myatt, A. A. Solodov, C. Stoeckl, B. Yaakobi, and D. H. Froula

University of Rochester
Laboratory for Laser Energetics

Outline

- Thomson-scattering experiments
- Simulations
- Hard x-ray measurements

Outline

- **Thomson-scattering experiments**
- Simulations
- Hard x-ray measurements

E24146a

Planar-target experiments were performed to observe TPD common electron plasma waves (EPW's) driven along the target normal

Experimental configuration

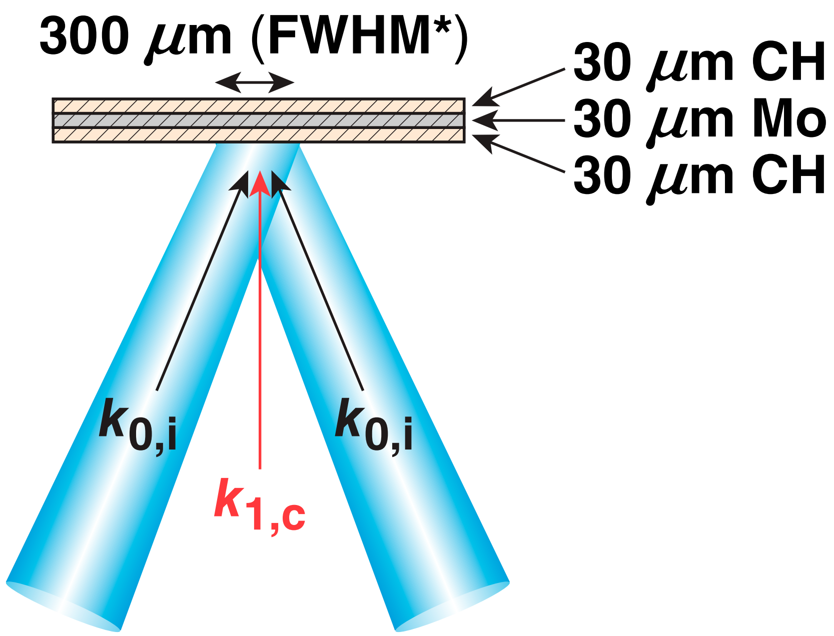

Five 3ω (351-nm) drive beams
0.75 kJ in 1 ns ($I_{overlap} = 8 \times 10^{14}$ W/cm^2)

Common-wave matching conditions**

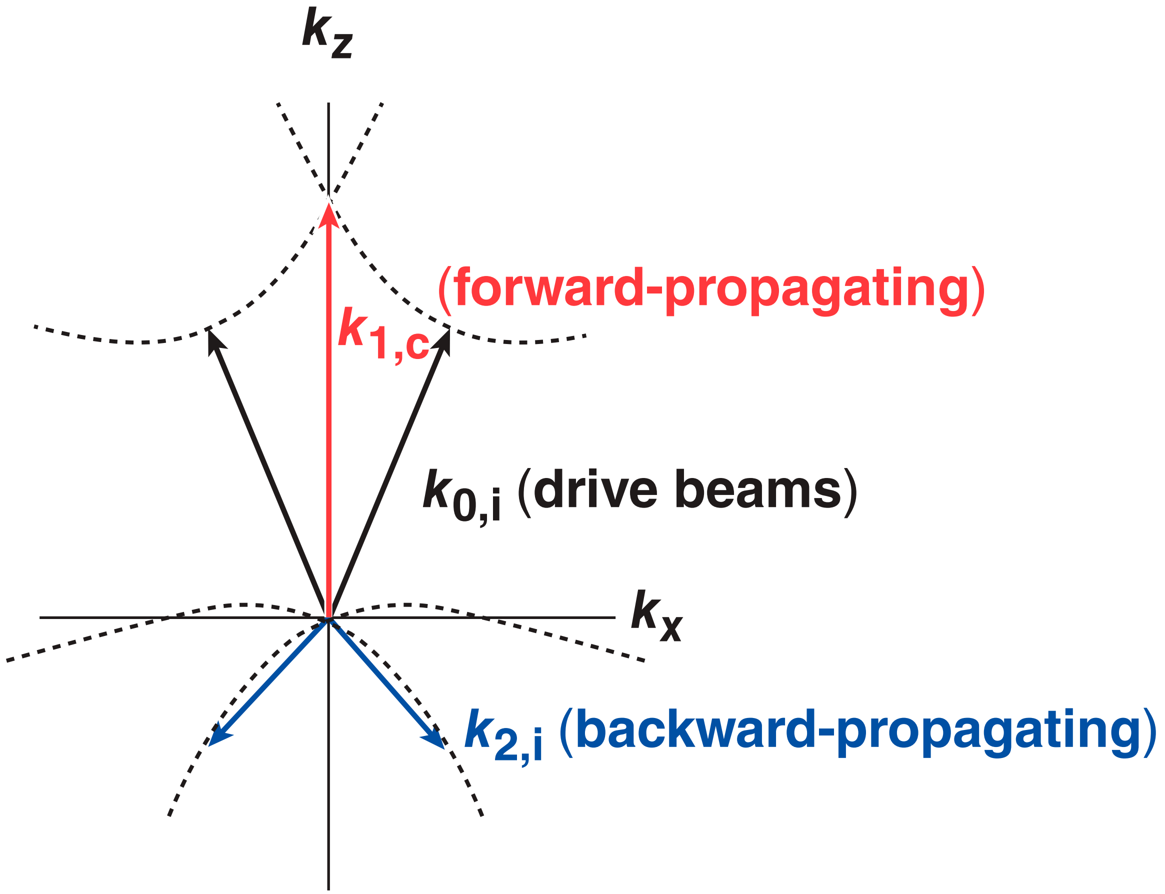

*FWHM: Full width at half maximum
**D. T. Michel *et al.*, Phys. Rev. Lett. 109, 155007 (2012).

E24211

Thomson scattering was configured to observe plasma waves along the target normal

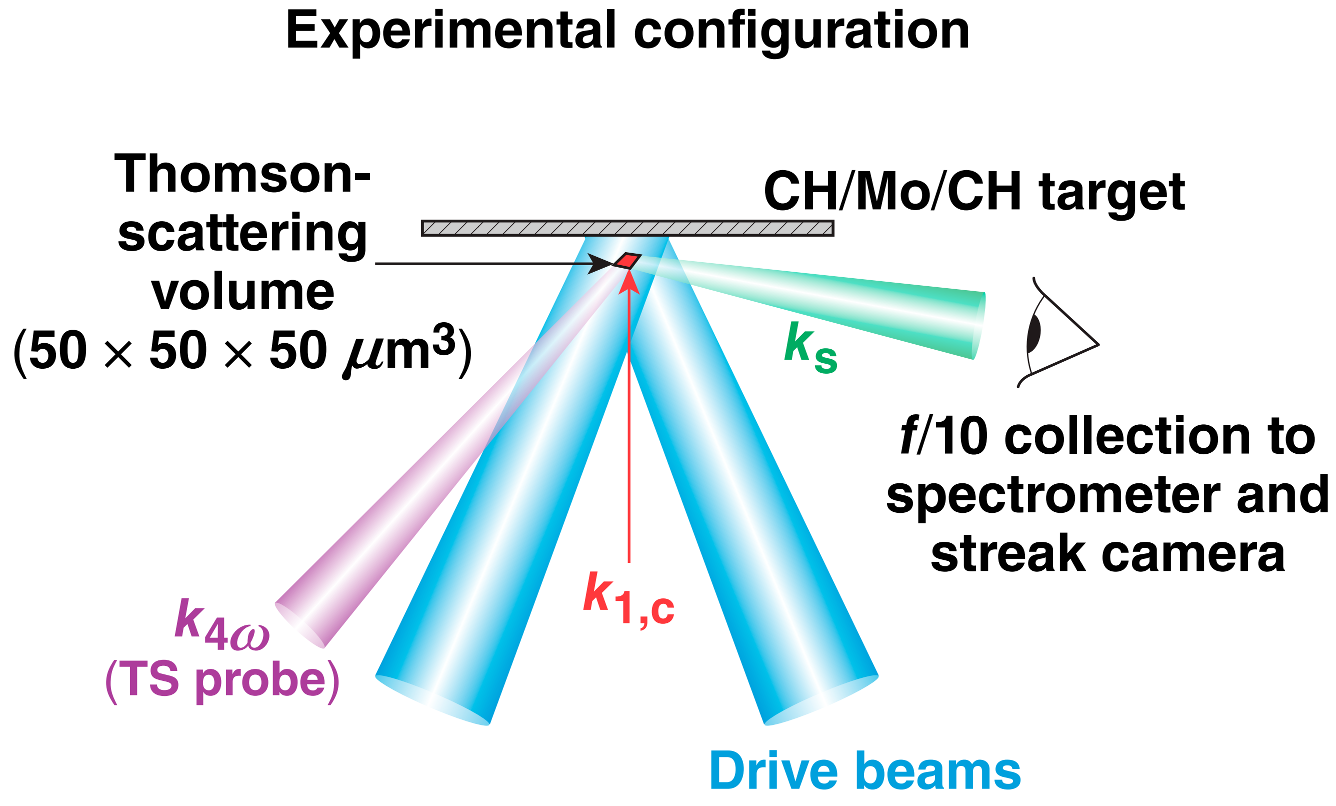

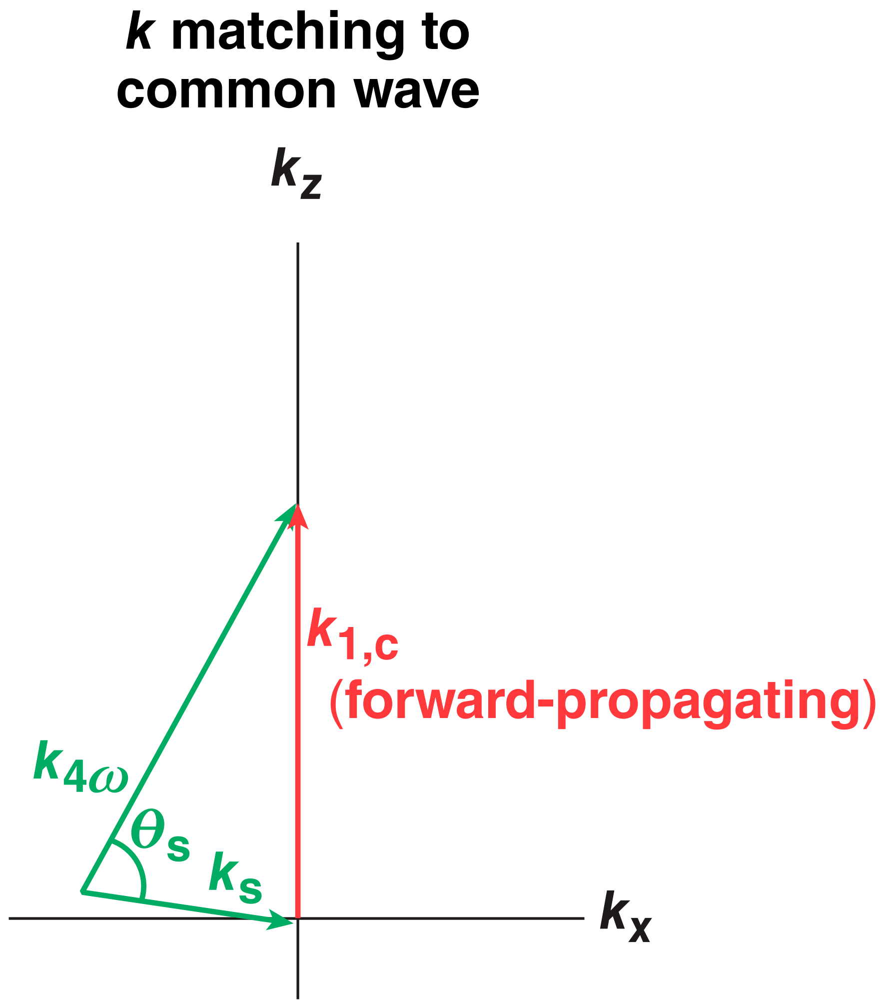

Thomson scattering was used to probe two different locations inside and outside the Landau cutoff

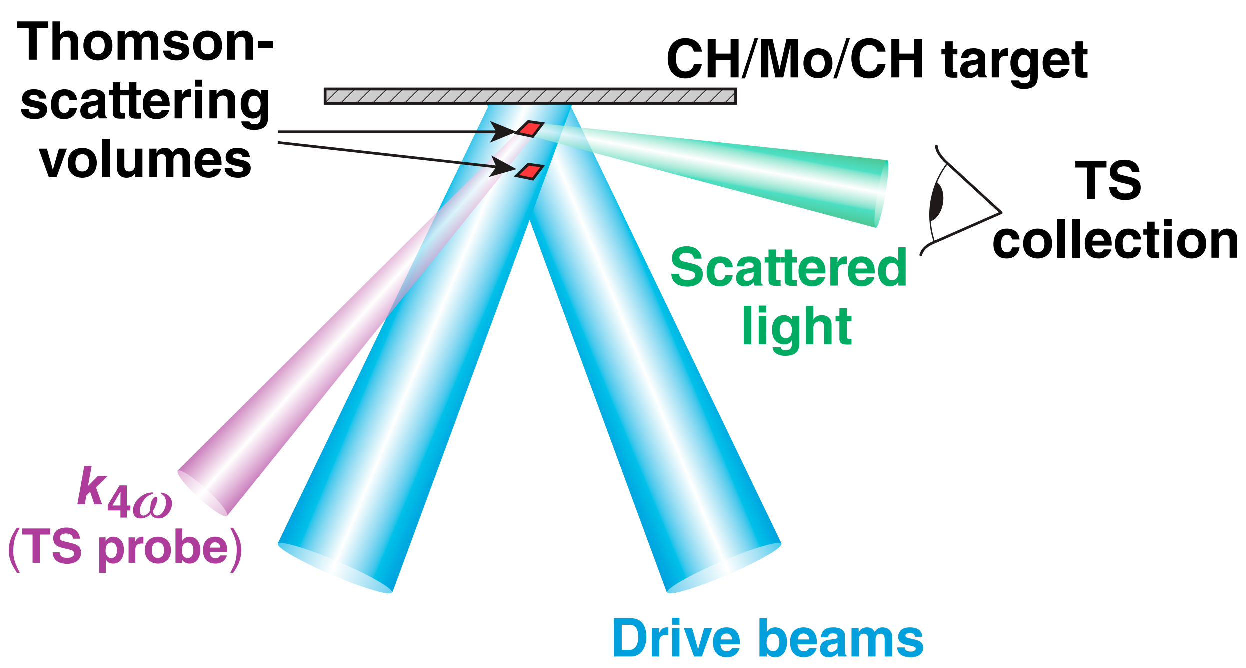

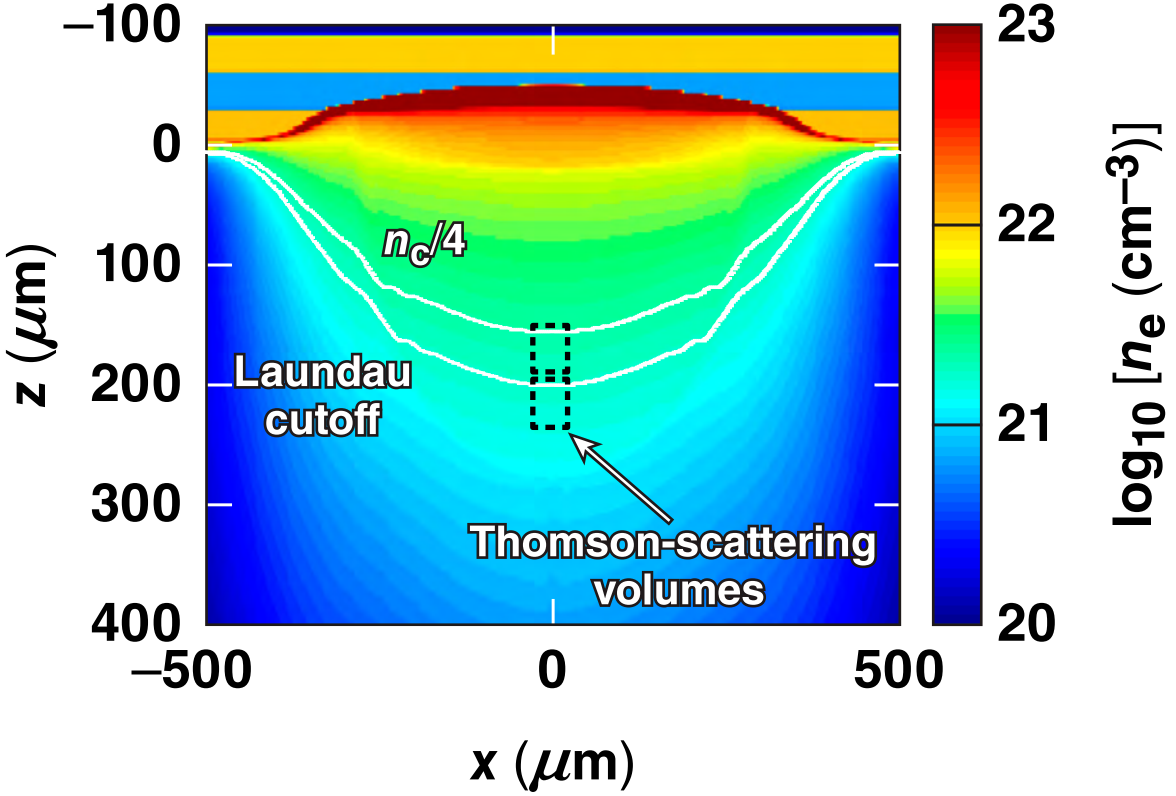

E24212

Large-amplitude TPD-driven waves were observed when probing inside of the Landau cutoff

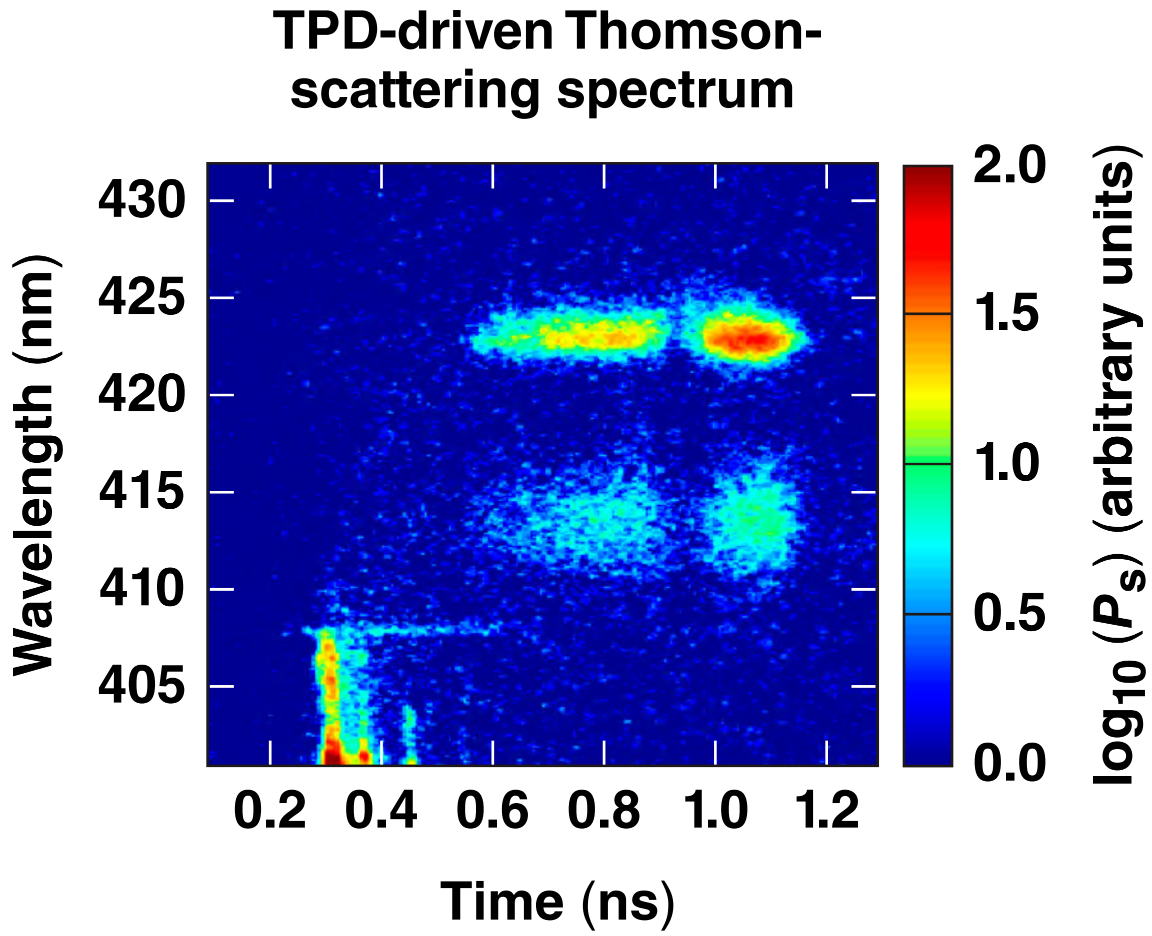

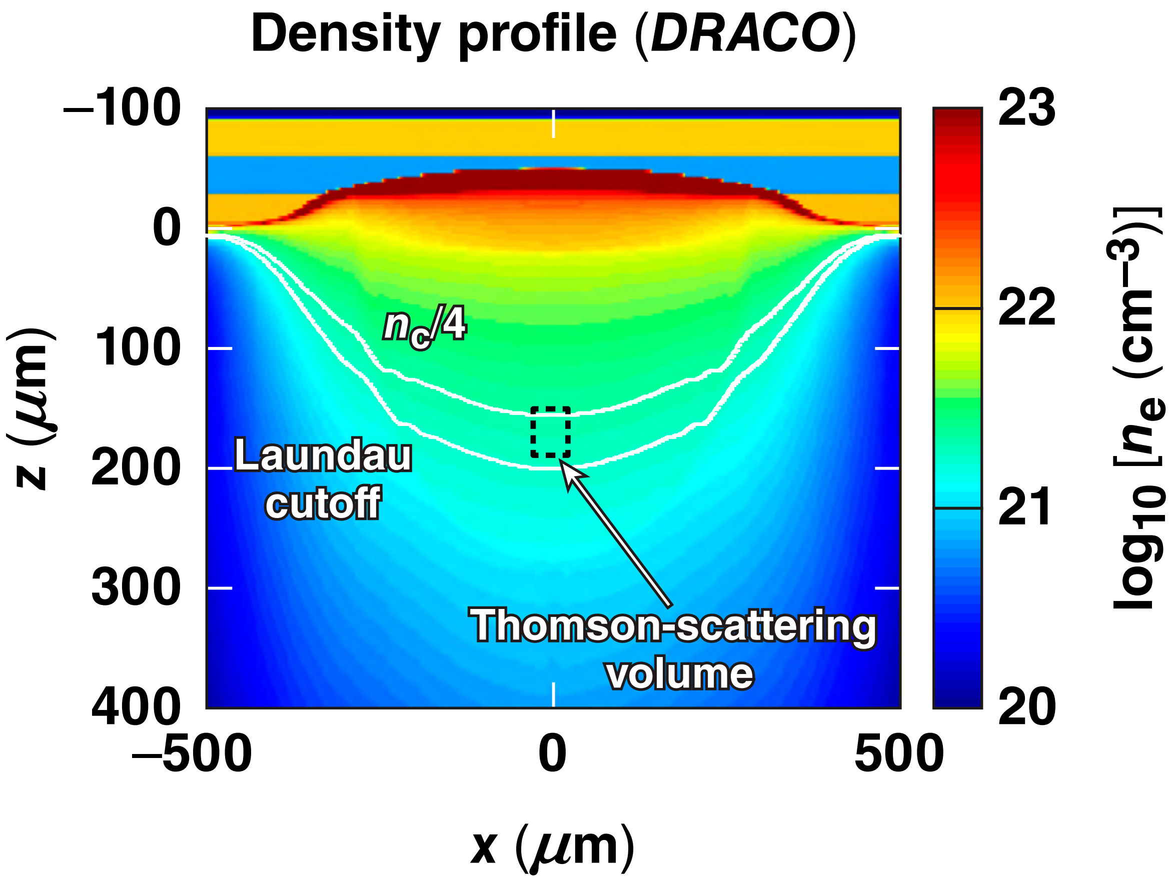

E24151

The TPD matching conditions restrict the wavelength of the Thomson-scattered light from forward-propagating EPW's to be greater than 423 nm

Forward-propagating

$$\omega_0 = \omega_1 + \omega_2 \begin{cases} \omega_1 = \omega_0/2 + \Delta \\ \omega_2 = \omega_0/2 - \Delta \end{cases}$$

Backward-propagating

$$\Delta_{min} \approx 3/8\,(k_0\lambda_{de})^2\omega_0$$

TPD-driven Thomson-scattering spectrum

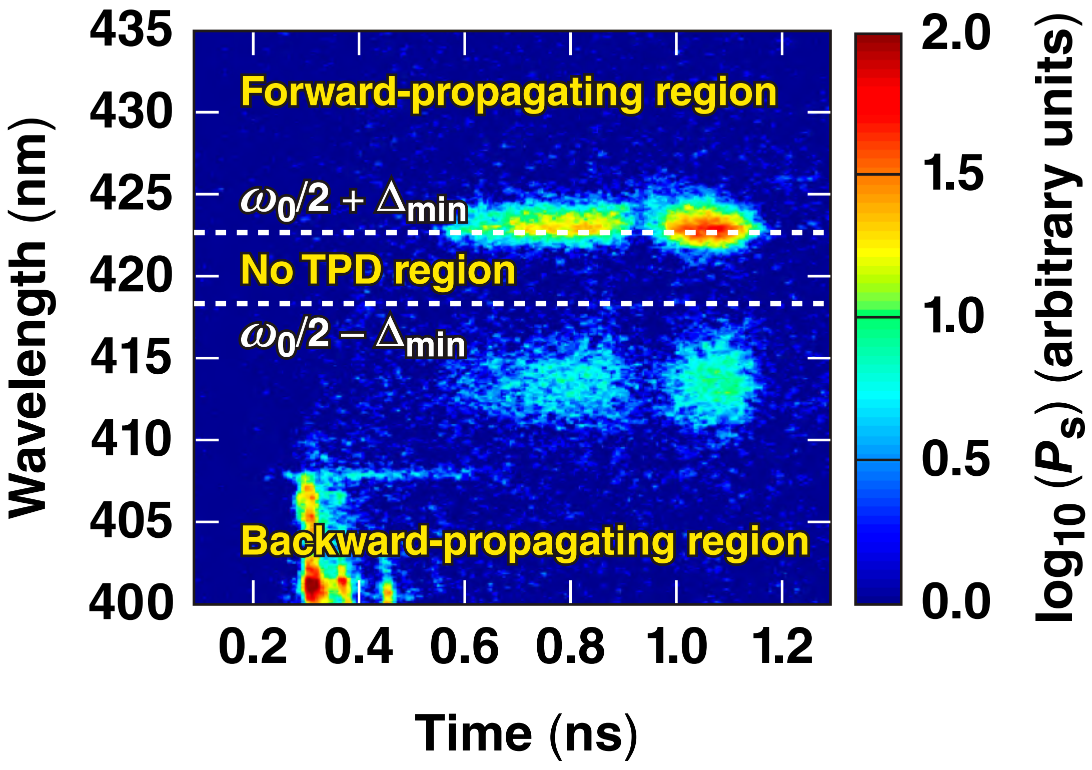

k matching to common wave

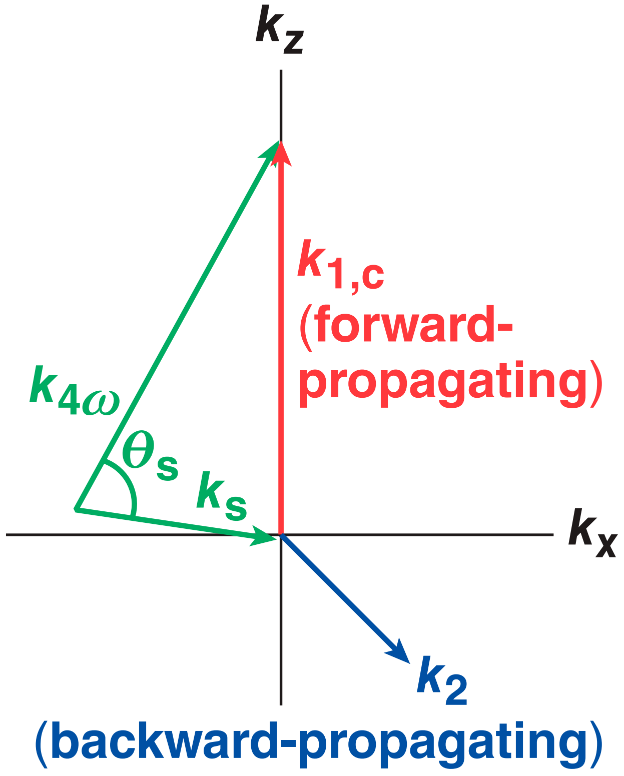

The lower-amplitude peak corresponds to wavelengths consistent with backward-propagating EPW's that are not directly observed by Thomson scattering.

E24213

The lower-amplitude peak corresponds to Langmuir decay of backward-propagating TPD waves

UR LLE

TPD-driven Thomson-scattering spectrum

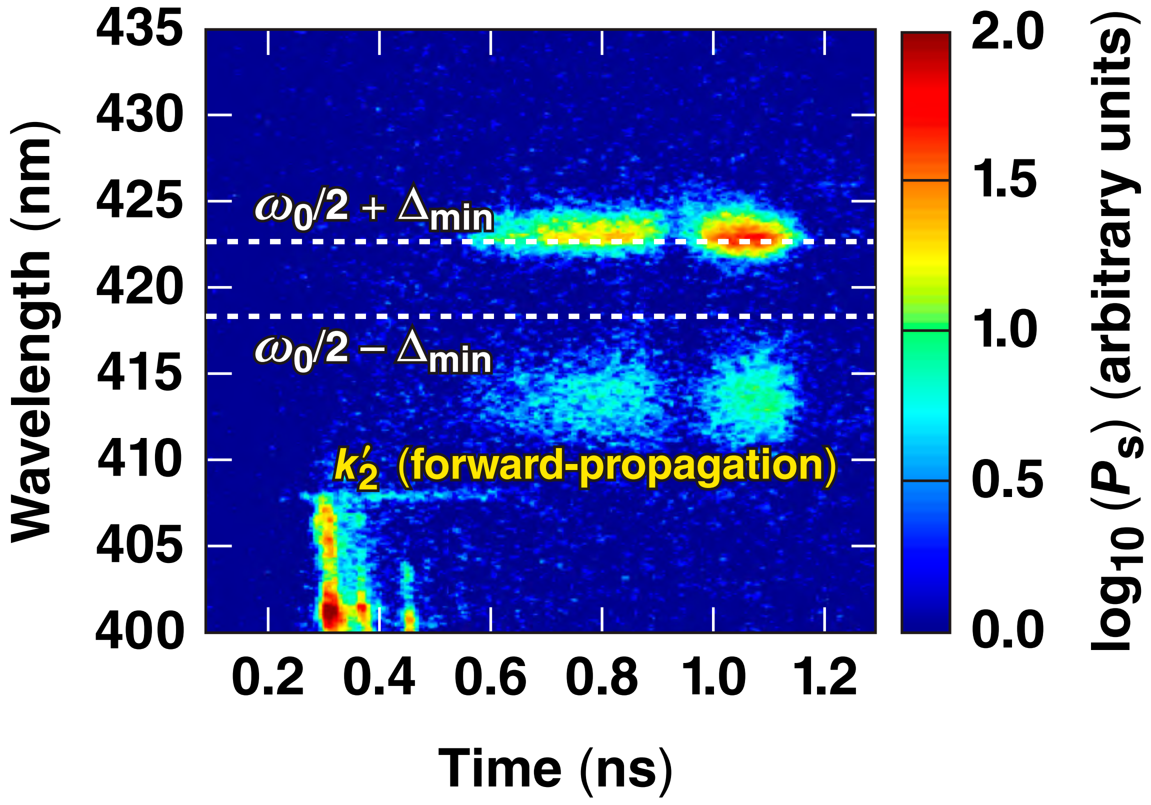

k **matching to Langmuir decay wave**

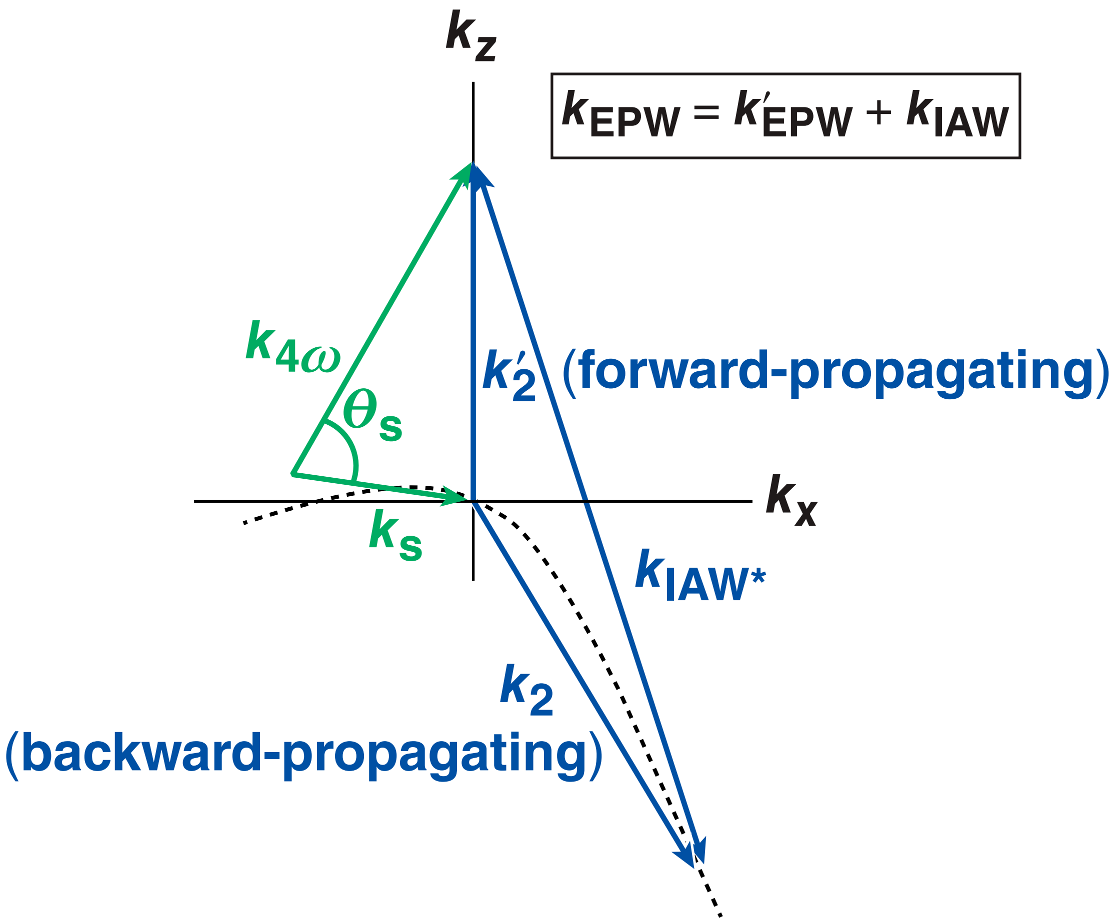

*IAW: ion-acoustic waves

E24152

Broad thermal Thomson-scattering features were observed when probing outside the Landau cutoff

Density profile (*DRACO*)

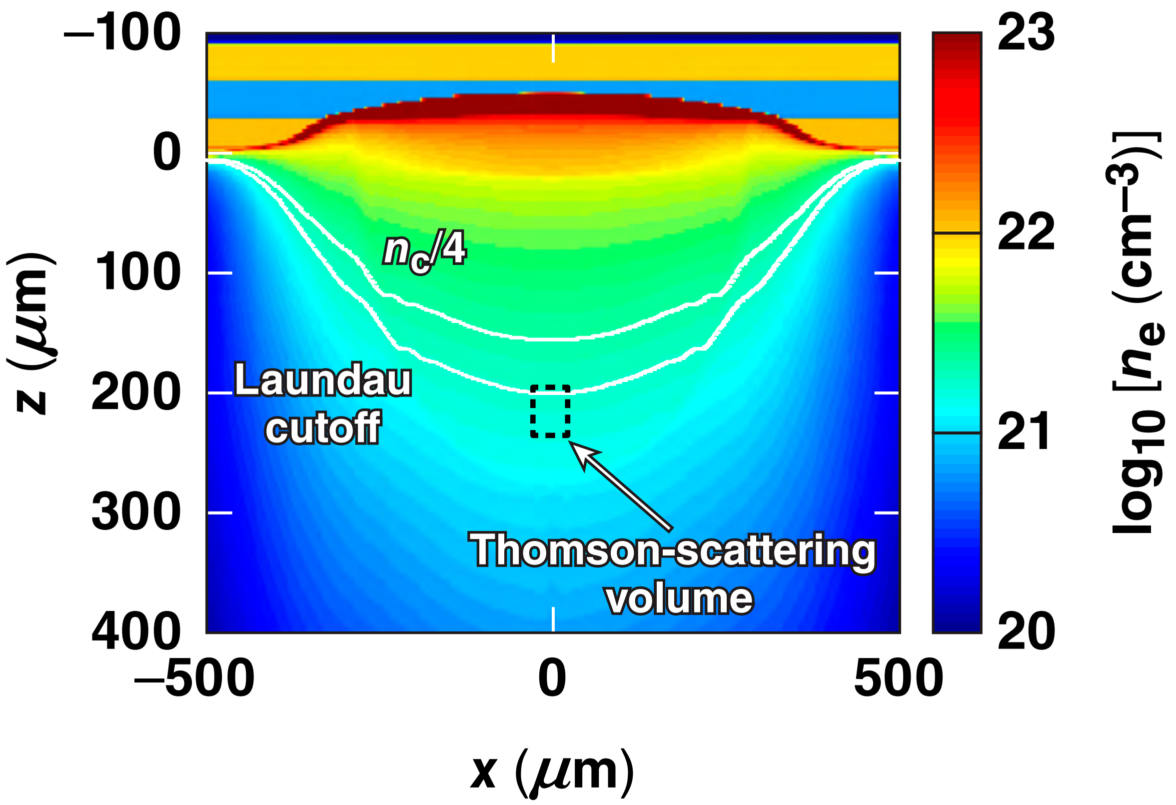

Thermal Thomson-scattering spectrum

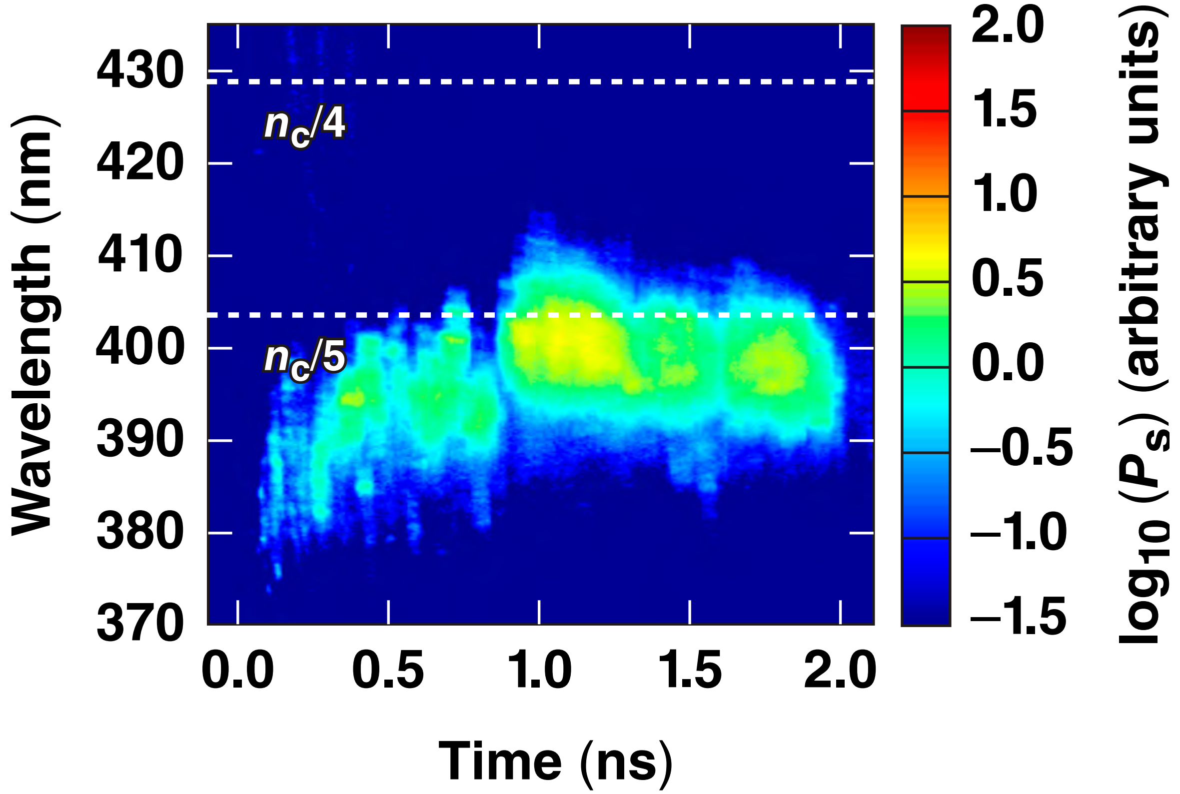

E24150

The common-wave peak is narrower than the thermal-scattering peaks, indicating a limited range of driven EPW's

Comparison of spectral lineouts (1.1 ns)

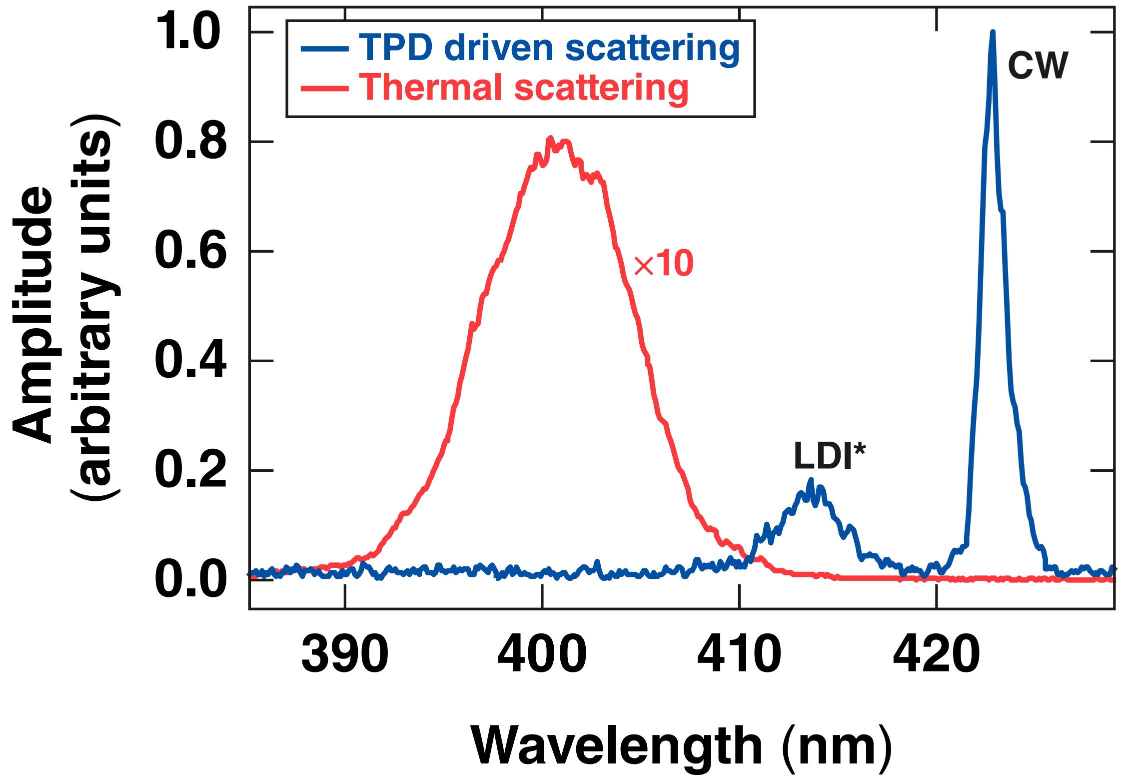

Five-beam linear growth rate in Thomson-scattering plane

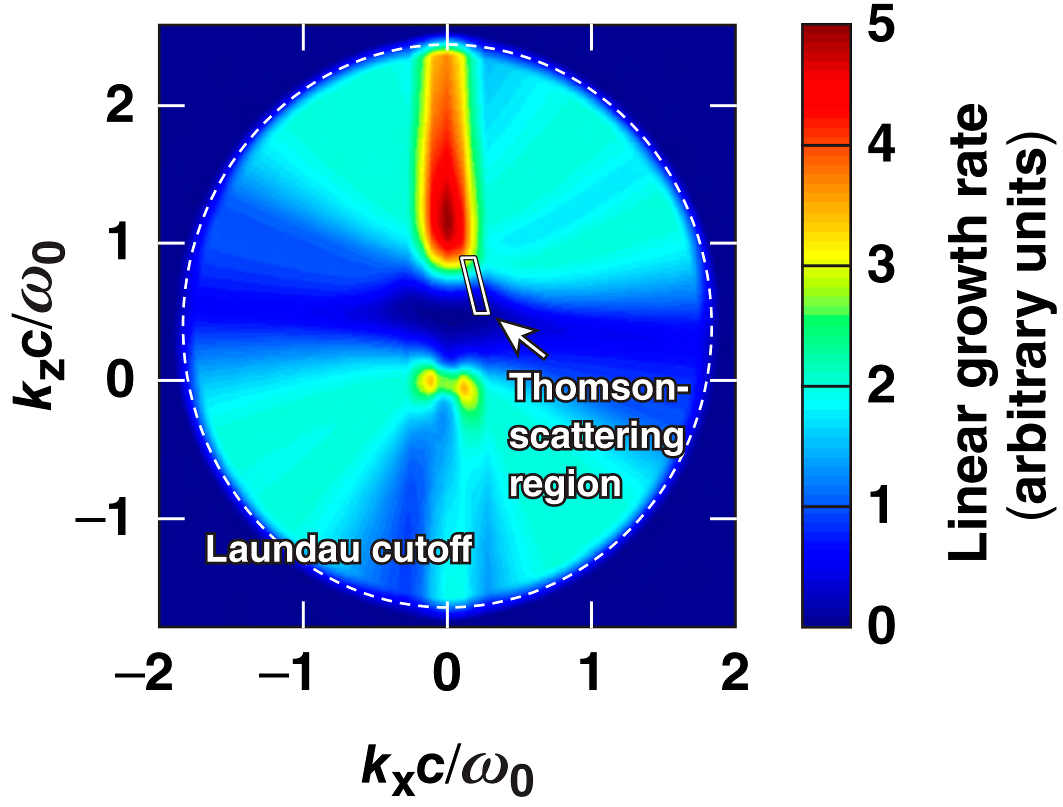

*LDI: Langmuir-decay instability

E24264

An alternate Thomson-scattering geometry probed a range of wave vectors where the common-wave matching conditions were not satisfied

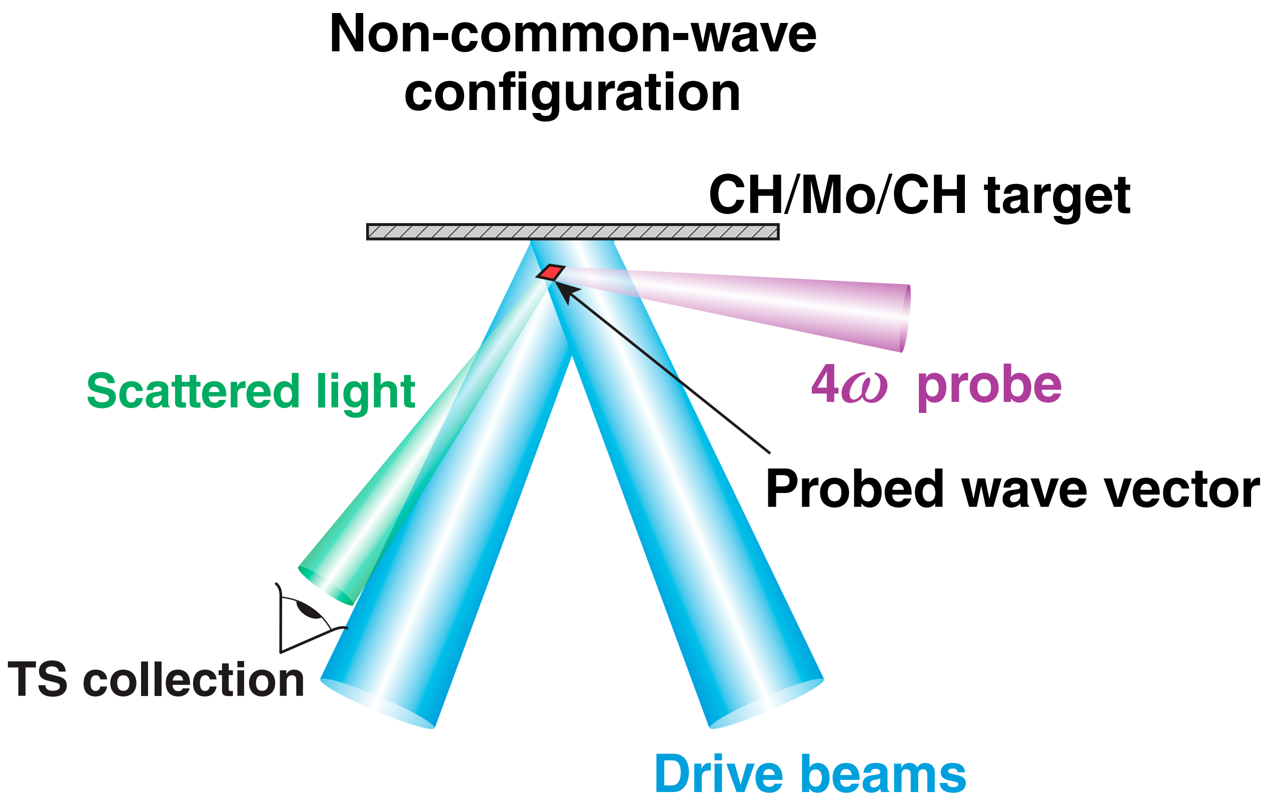

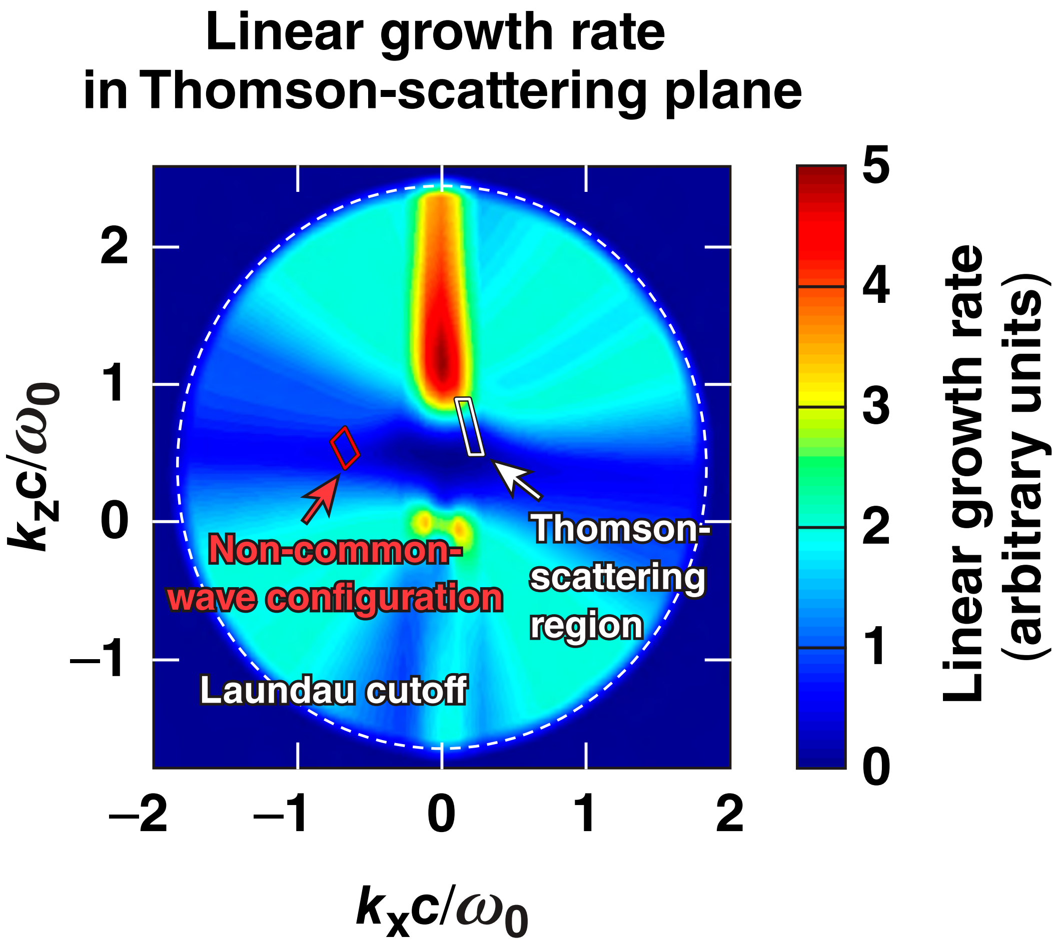

E24265

Large-amplitude TPD and Langmuir-decay–driven waves were observed in the non-common-wave scattering configuration

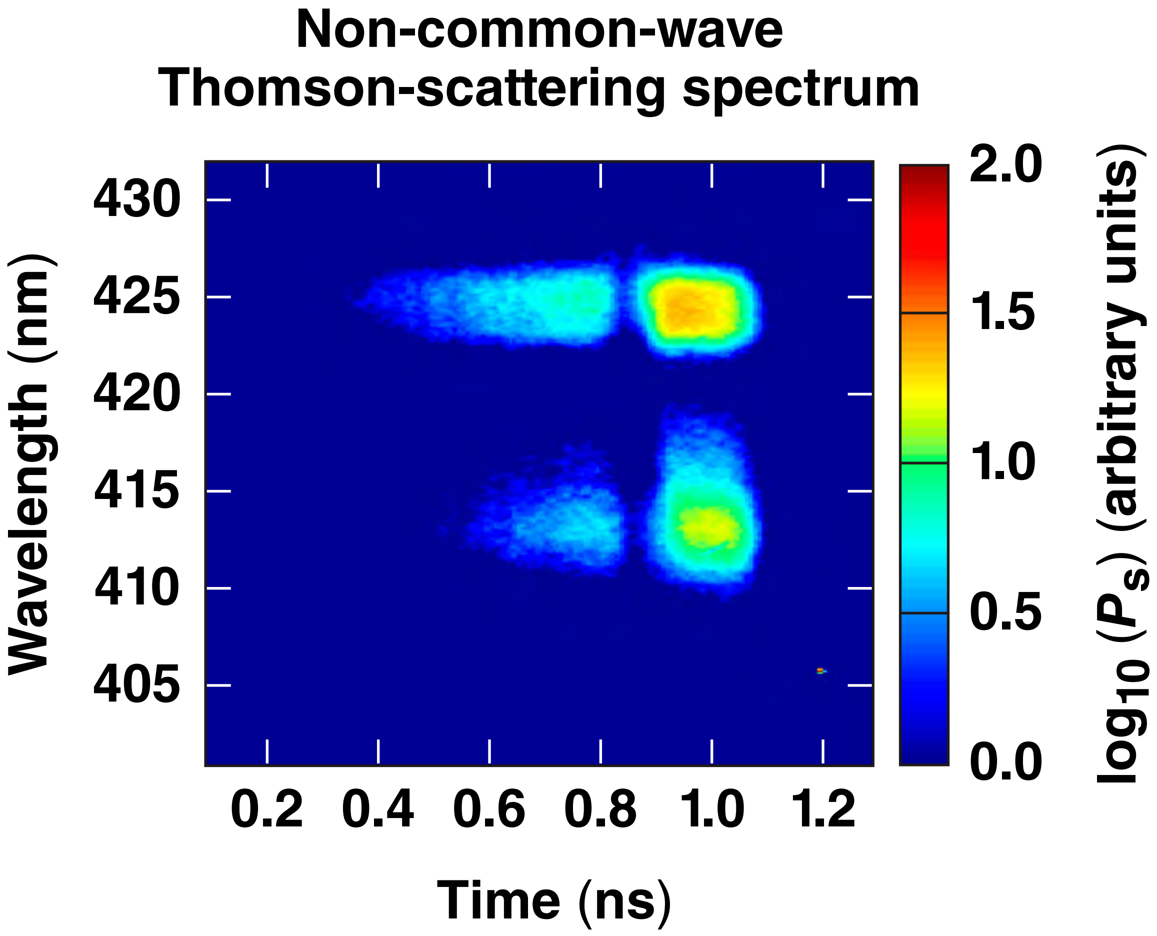

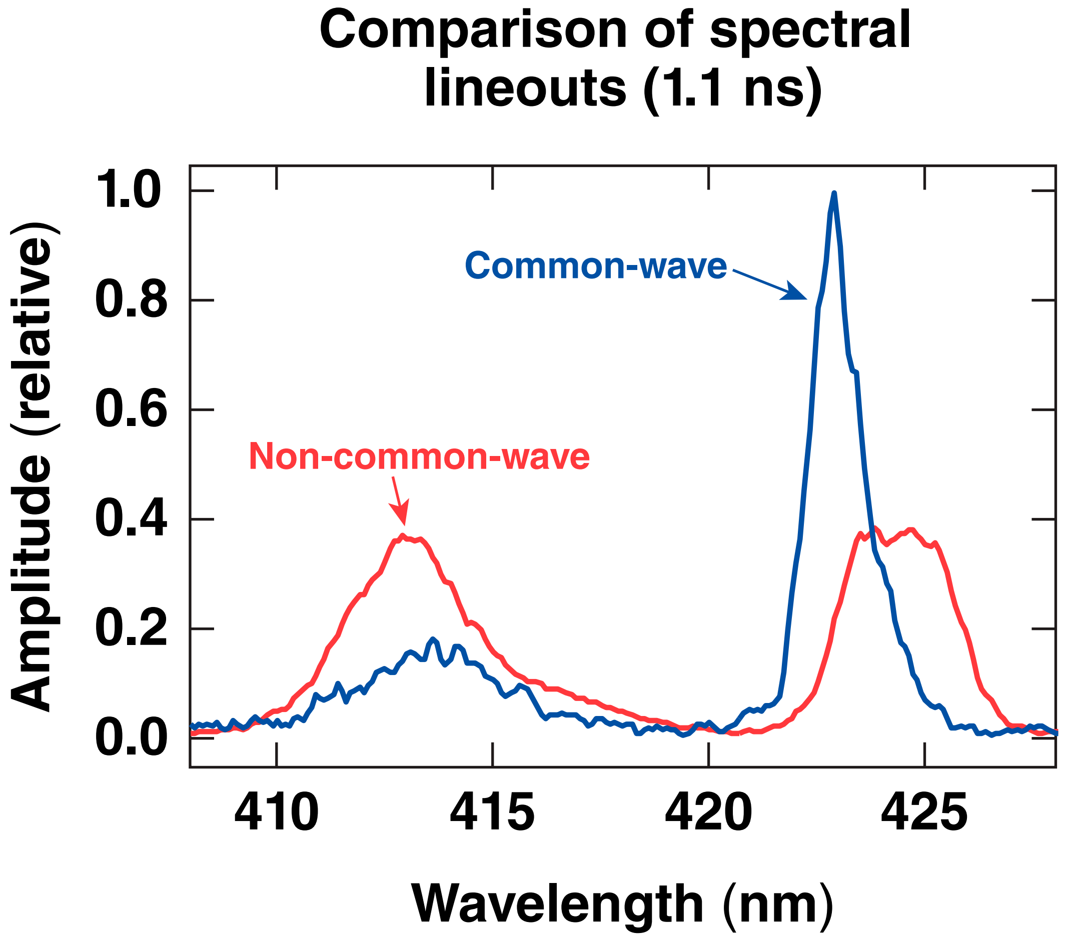

The observation of TPD and Langmuir-decay–instability driven waves in the non-common-wave geometry indicates a broad spectrum (*k* space) of driven waves.

E24153

Outline

- Thomson-scattering experiments
- **Simulations**
- Hard x-ray measurements

Three-dimensional simulations were required to capture the multibeam geometry and turbulent nature of the plasma instabilities

*LPSE** uses an established model that includes

- Experimental beam geometry
- Three-wave interactions
  - two-plasmon decay
  - Langmuir decay
  - modulational instability
- Strong turbulence
  - cavitation
  - collapse
- Hybrid-particle model
  - electron-velocity distribution
  - nonlinear Landau damping

LPSE geometry

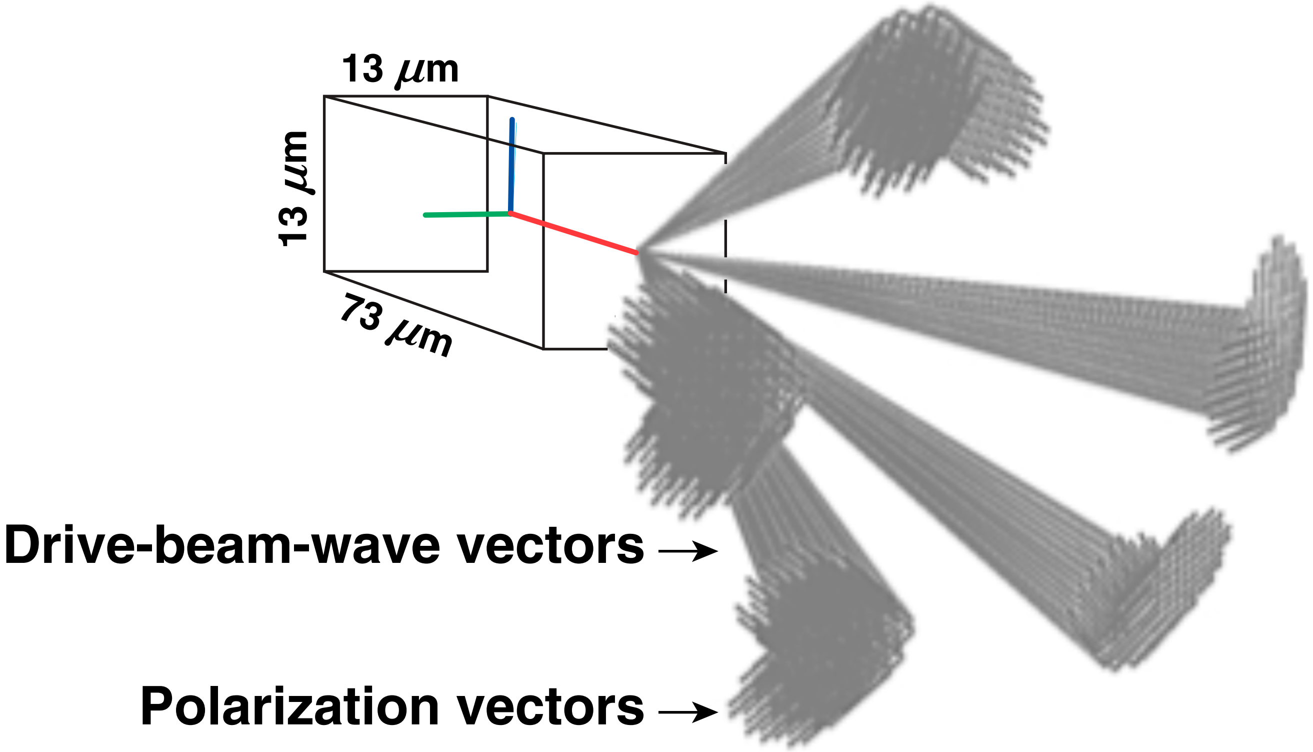

*J. F. Myatt, this conference

E24266

LPSE solves a pair of equations that model the coupling between the envelope of high-frequency-electrostatic perturbations and low-frequency-density perturbations*

$$\overbrace{\nabla \cdot \left[2i\omega_{\mathrm{pe}}(\partial_t + \underbrace{\nu_{\mathrm{e}}}_{\text{Hybrid-particle evolution}}) + 3v_{\mathrm{te}}^2\nabla^2 - \omega_{\mathrm{pe}}^2 \frac{\delta N}{n_0}\right]}^{\text{EPW propagation in an inhomogeneous plasma}} \vec{E} = \overbrace{\omega_{\mathrm{pe}}^2 \nabla \cdot \left(\frac{\delta n}{n_0}\vec{E}\right)}^{\text{Coupling to ions}} + \overbrace{\frac{e}{4m_{\mathrm{e}}}\nabla \cdot \left[\nabla\left(\vec{E}_0 \cdot \vec{E}^*\right) - \vec{E}_0 \nabla \cdot \vec{E}^*\right]}^{\text{Coupling to drive beams}} + \underbrace{S_E}_{\text{Thermal fluctuations}}$$

$$\underbrace{\left[\partial_t^2 + 2\nu_{\mathrm{i}}\nabla_t - c_s^2\nabla^2\right]\delta n}_{\text{IAW propagation}} = \underbrace{\frac{\nabla^2\left|\vec{E} + \vec{E}_0\right|^2}{16\pi m_{\mathrm{i}}}}_{\text{Ponderomotive force}} + \overbrace{S_{\delta n}}^{\text{Thermal fluctuations}}$$

*D. A. Russell and D. F. DuBois, Phys. Rev. Lett. 86, 428 (2001).

E24154

The hybrid-particle model uses the longitudinal fields to accelerate electrons and modify the electron-velocity distribution

- Electron trajectories are solved exactly using the electrostatic potentials
- The electron-velocity distribution is used to calculate Landau damping

Electron-energy distribution

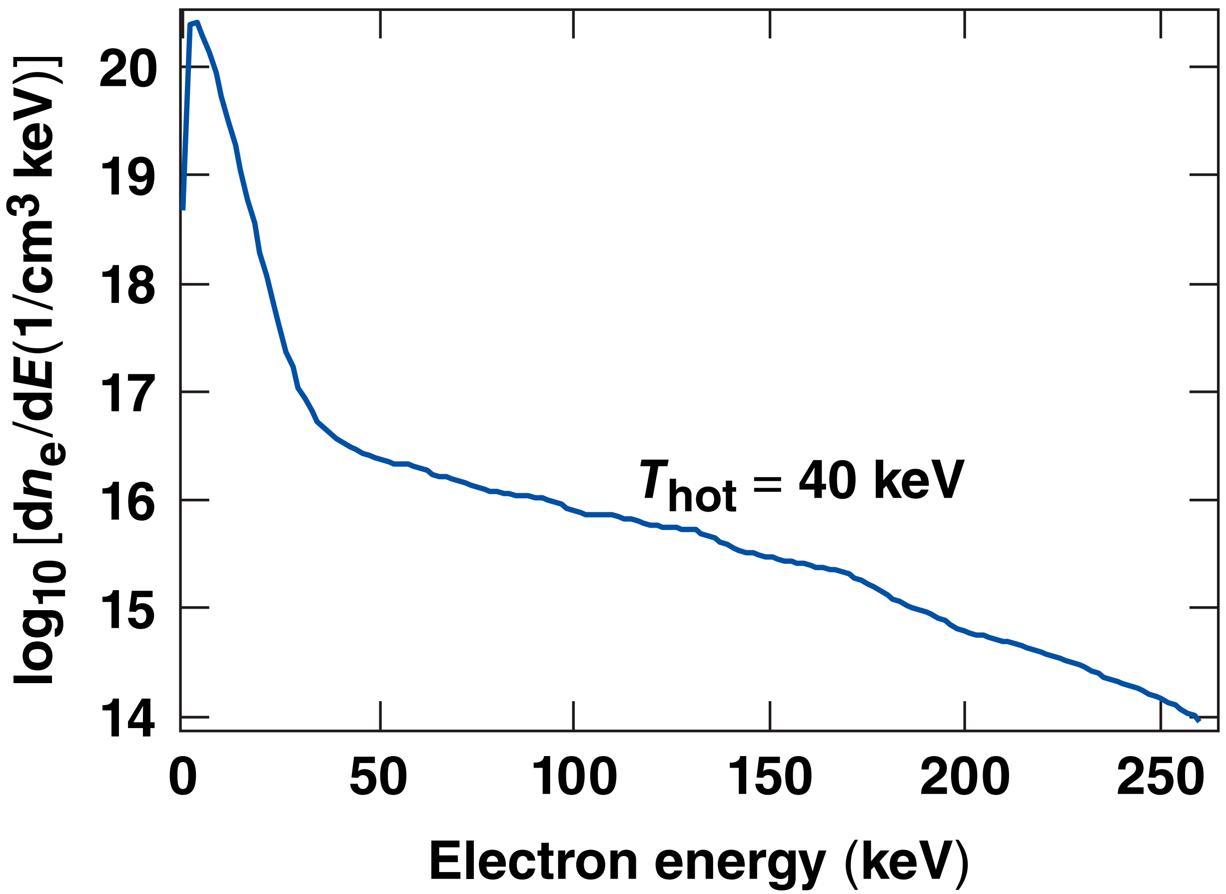

E24157

LPSE simulated the region of the plasma observed with Thomson scattering

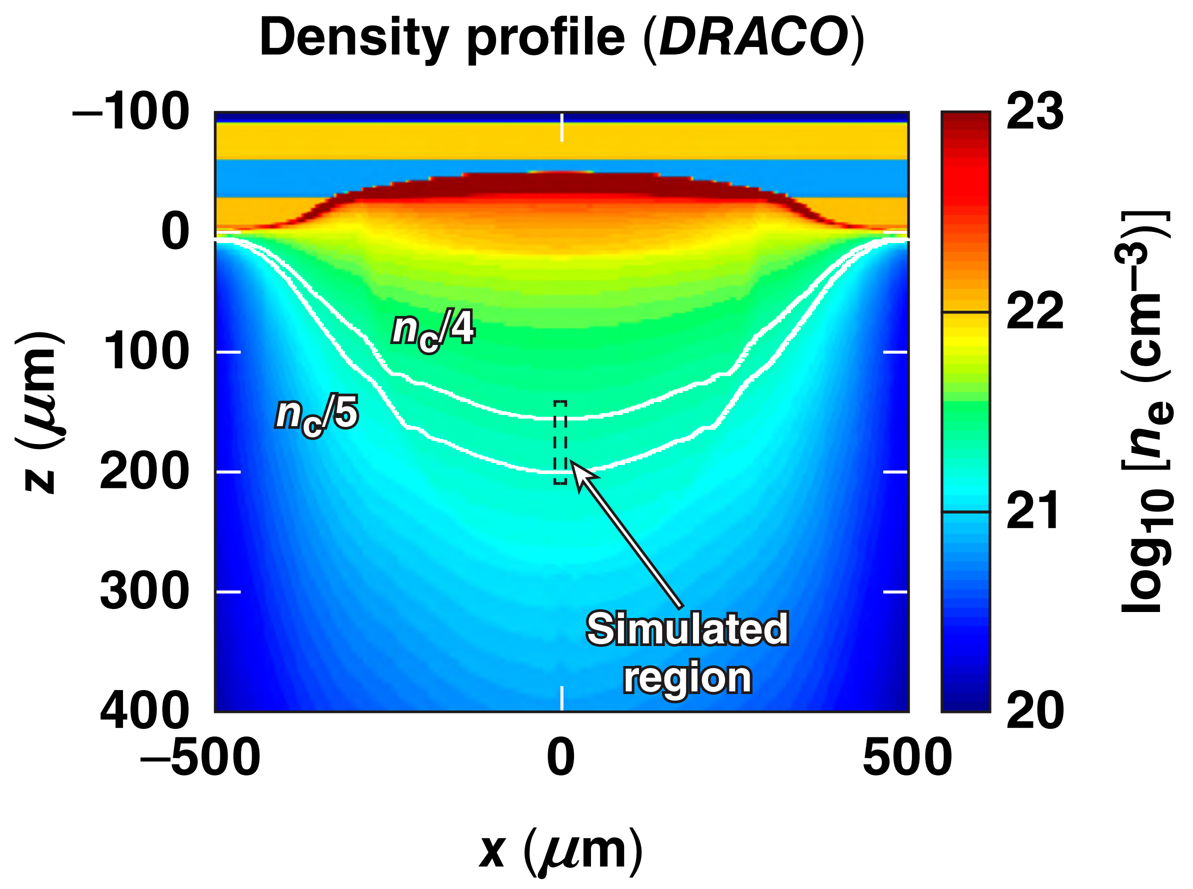

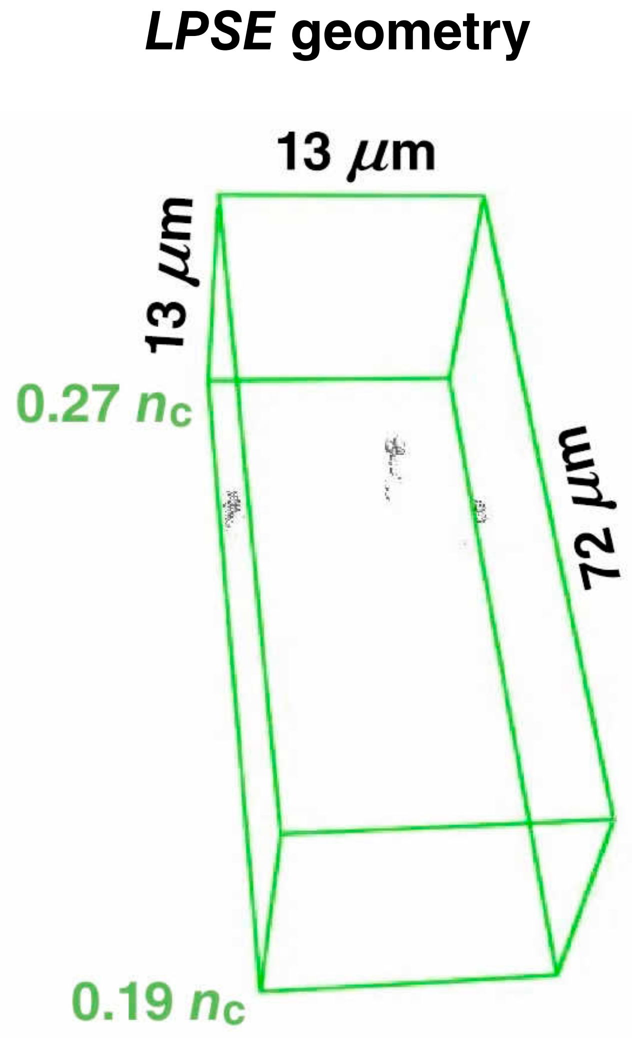

E24214

LPSE simulations predict a broad spectrum of driven EPW's

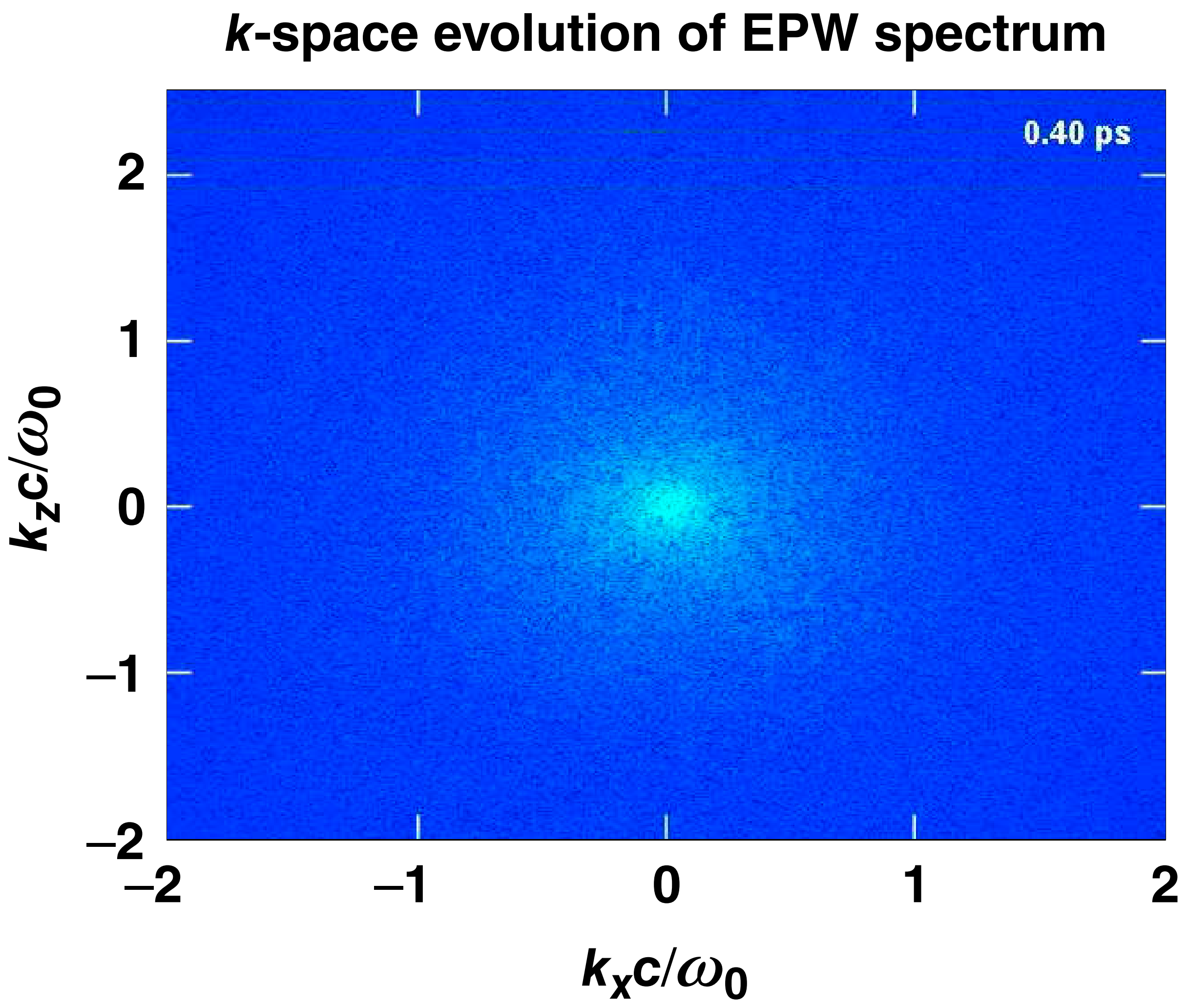

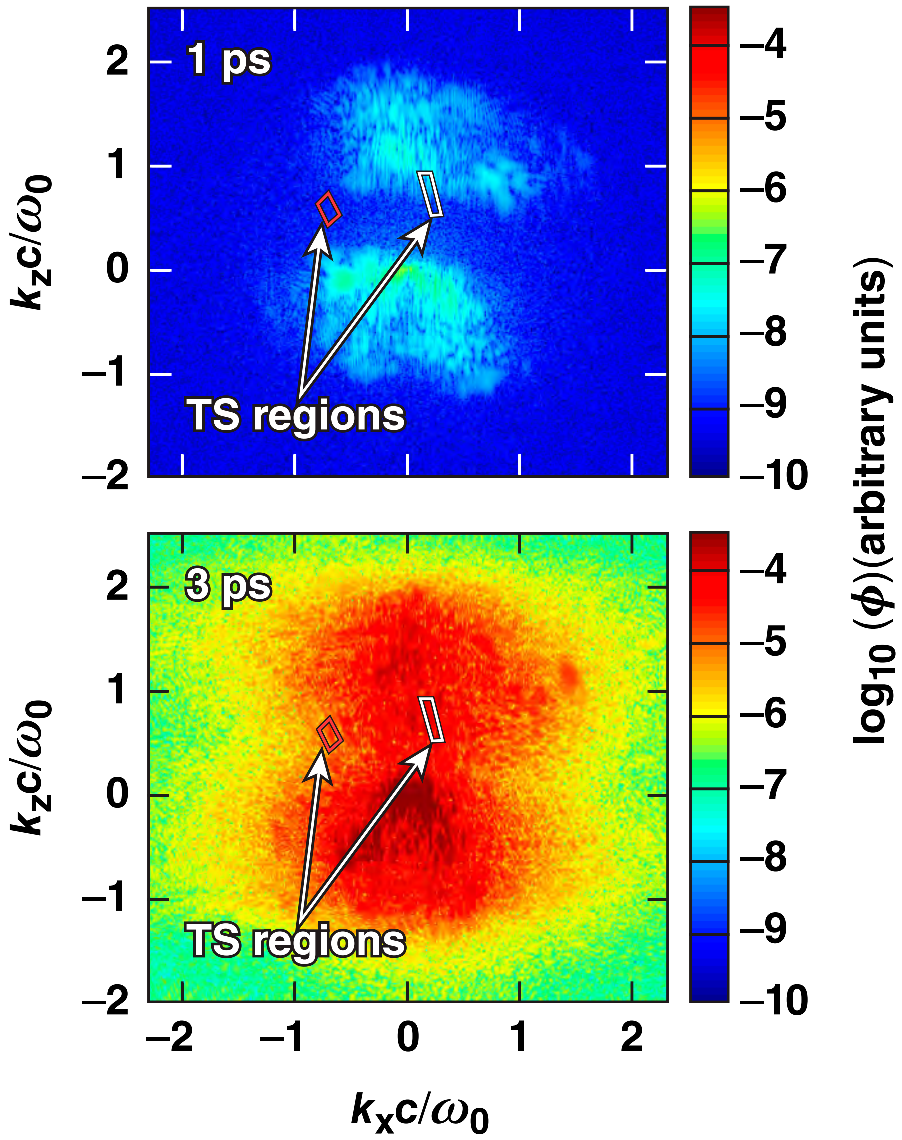

E24215

Simulated scattering spectra from *LPSE* reproduce the observed scattering peaks in both Thomson-scattering configurations

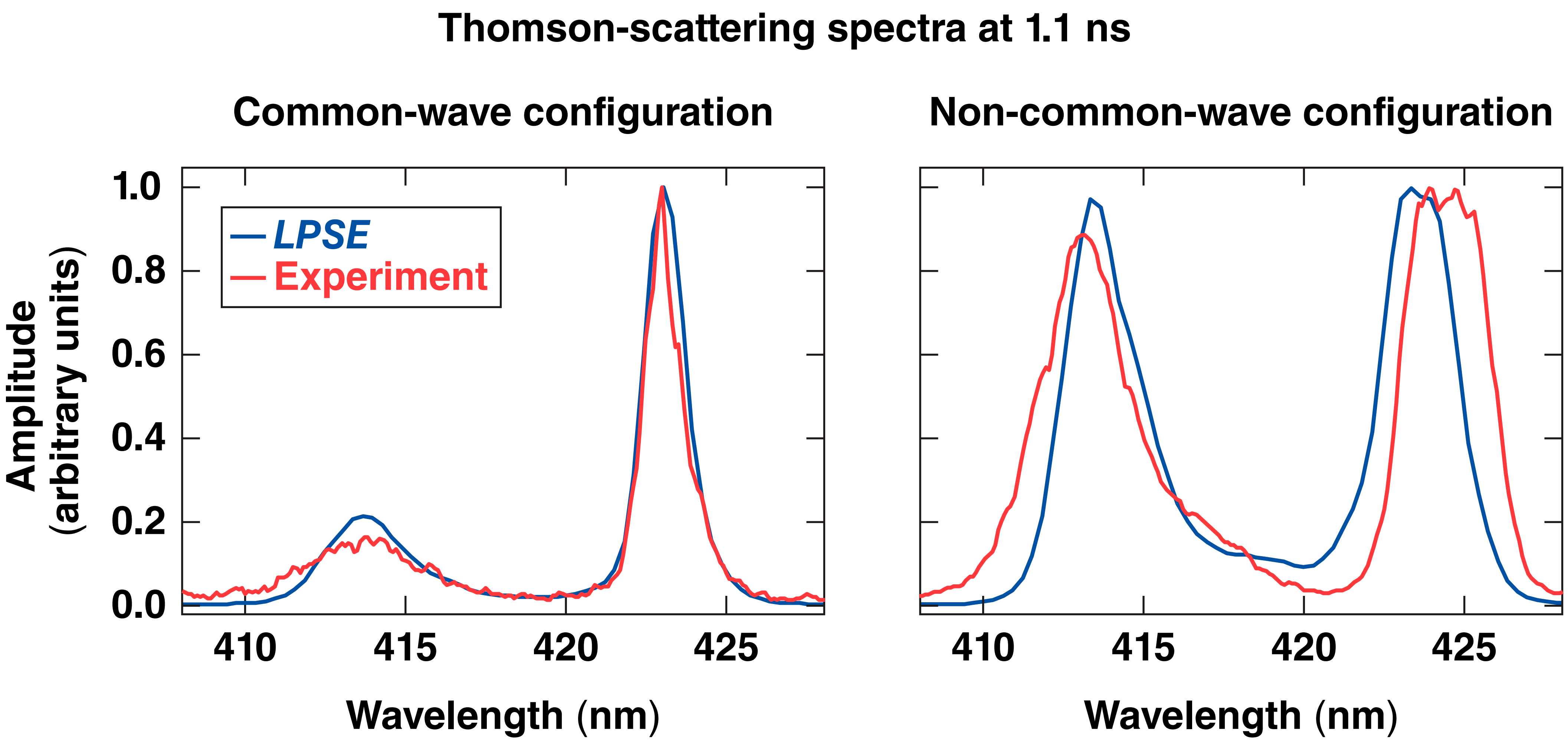

*R. K. Follett *et al.*, Phys. Rev. E 91, 031104 (2015).

E24155

Outline

- Thomson-scattering experiments
- Simulations
- **Hard x-ray measurements**

E24146c

Hard x-ray detectors were used to measure the hot-electron distribution

Experimental configuration

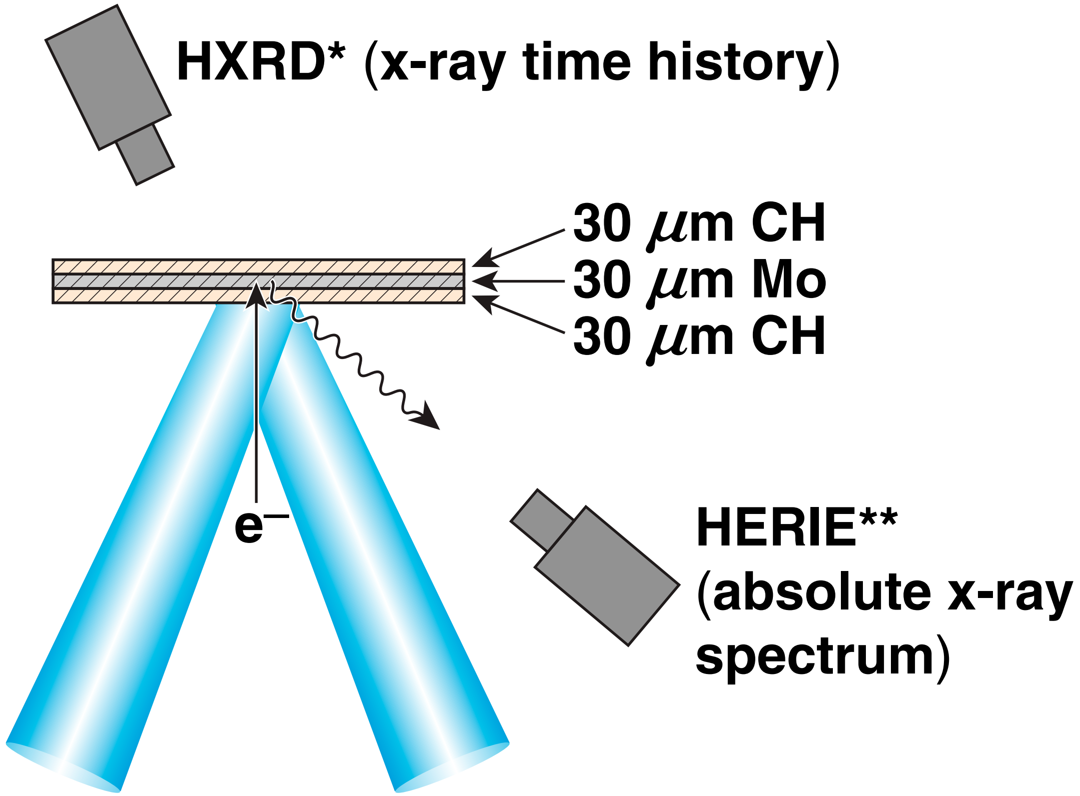

*HXRD: Hard x-ray detector
**HERIE: High-energy–radiography imager

E24267

The HERIE channels were fit to the spectral flux calculated using Monte Carlo simulations of a Maxwellian electron energy distribution

$$PSL_{\text{hot,i}} = n_e \sqrt{\frac{32}{\pi m_e}} \int dt \int dA \int d\Omega \int S_i(E) M_{e \to \gamma}(E,\Omega) \frac{E}{T_{\text{hot}}^{3/2}} e^{-E/T_{\text{hot}}} dE$$

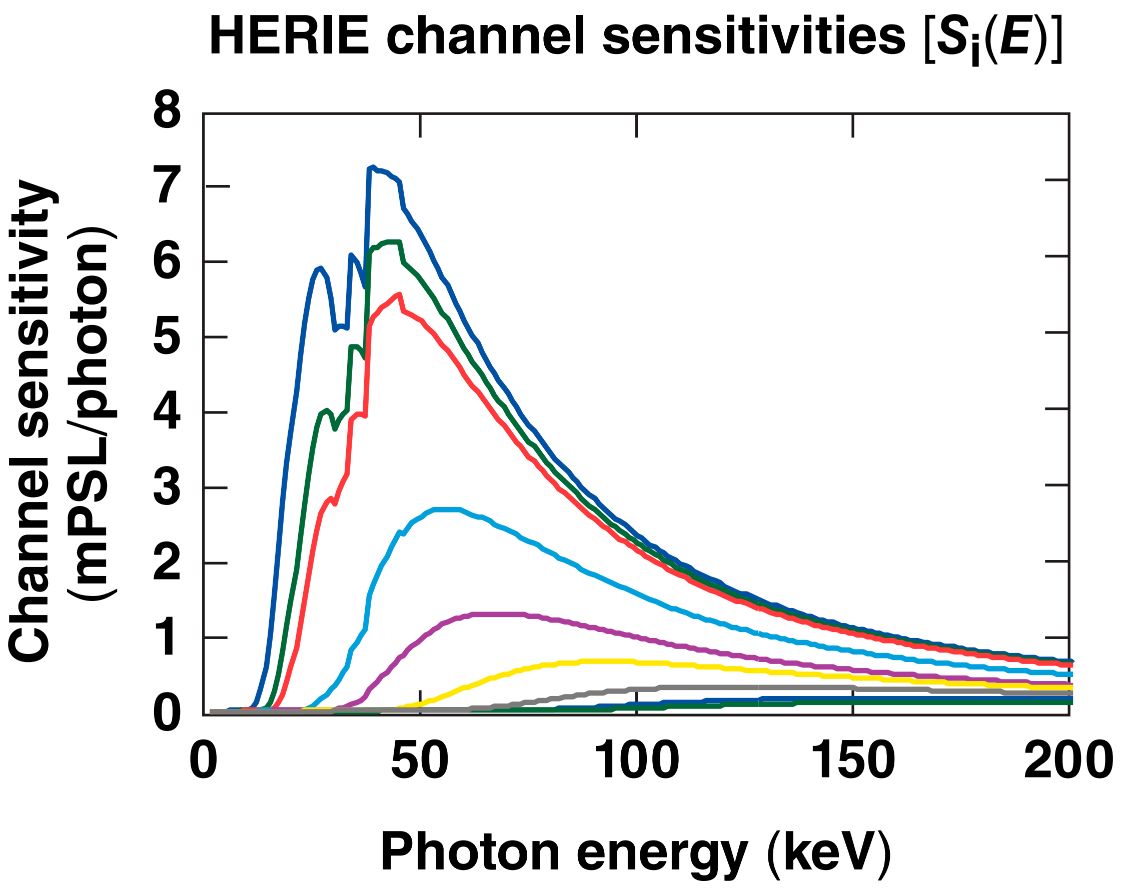

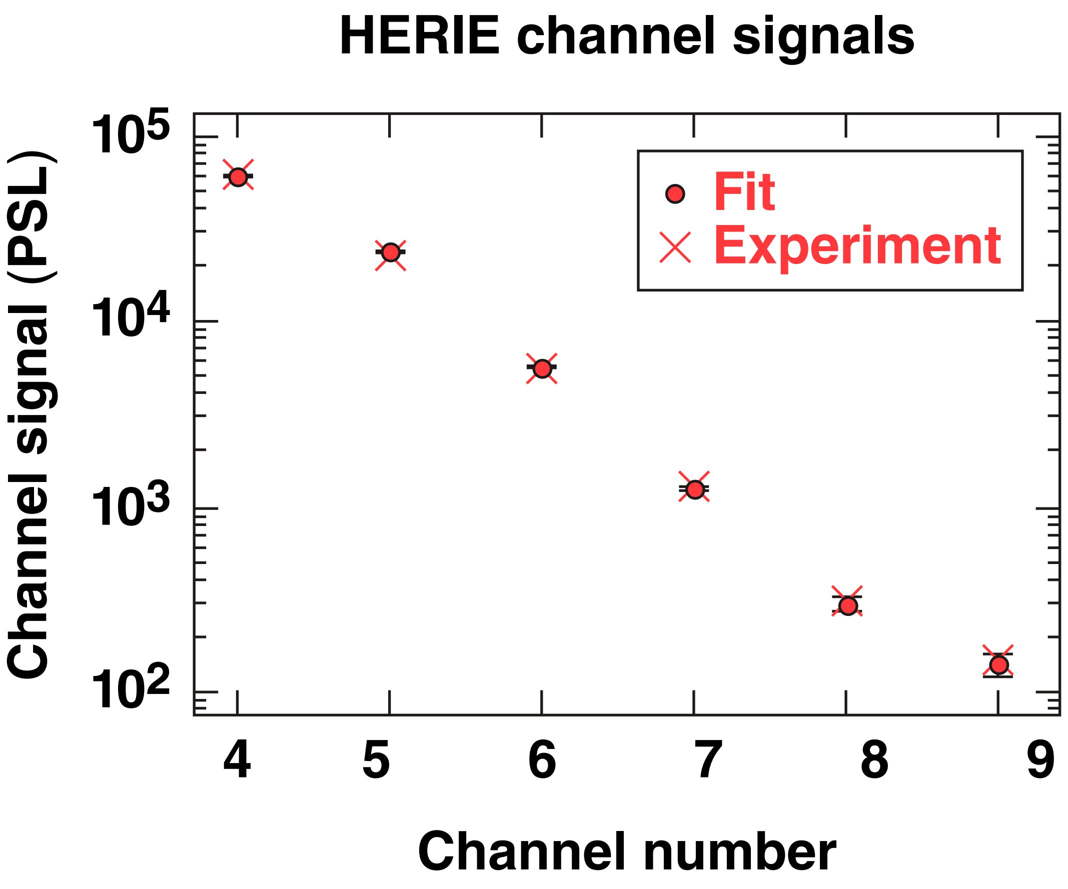

E24268

To make a direct comparison between hot-electron measurements and simulations, it is necessary to account for spatial and temporal variations present in the experiment

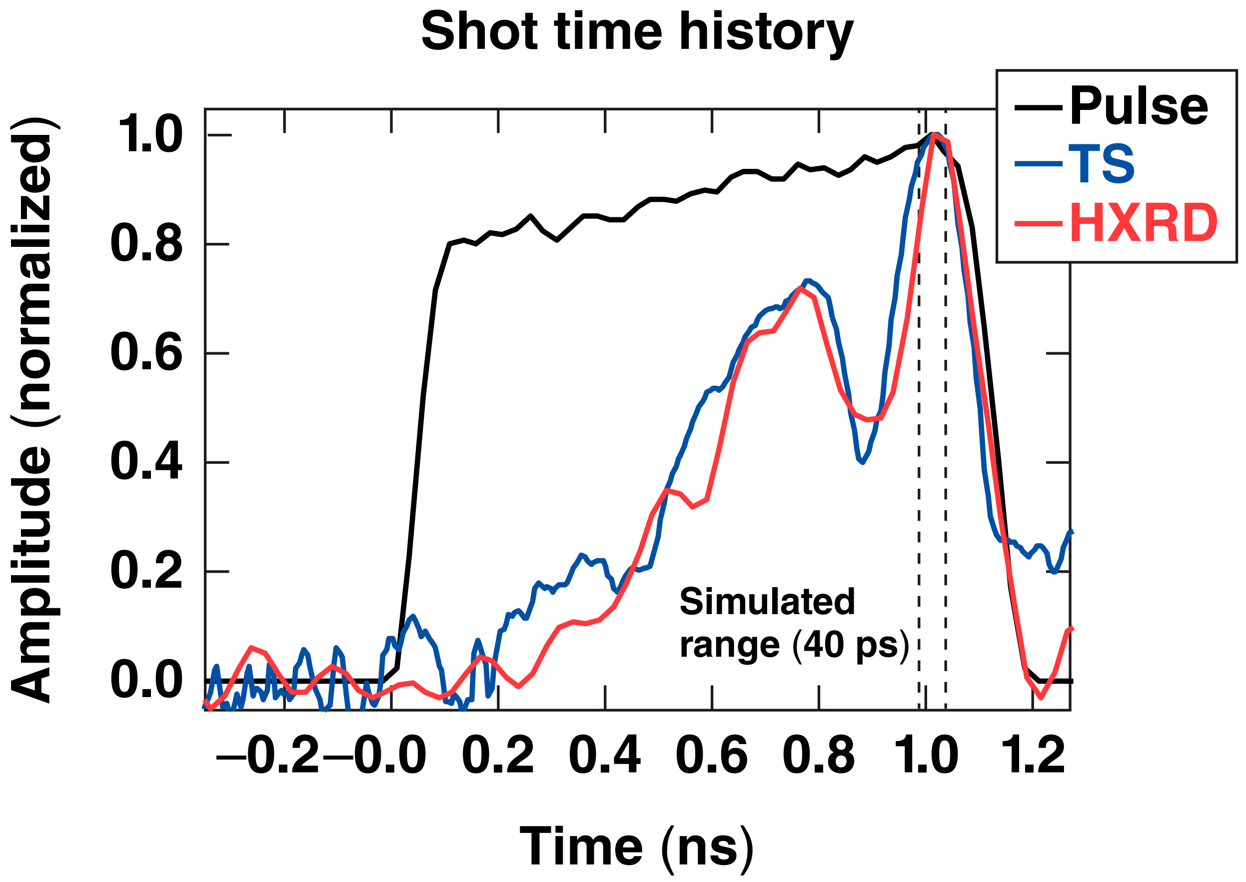

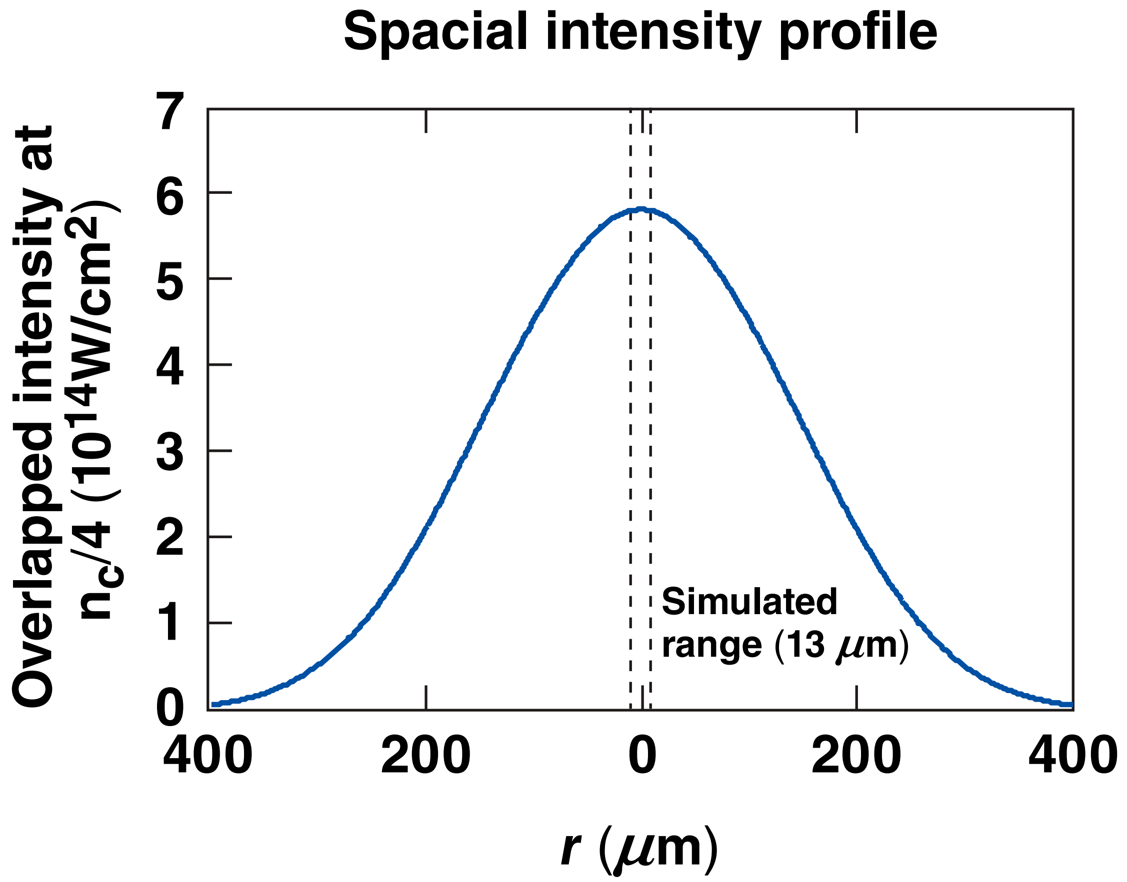

E24269

A series of *LPSE* runs combined with hydrodynamic predictions from *DRACO* were used to calculate an expected hot-electron fraction

LPSE hot-electron fraction conversion

$$\langle F_{hot} \rangle = \frac{\int dt \int F_{hot}^{LPSE}(r,t) I(r,t) r dr}{\int dt \int I(r,t) r dr}$$

DRACO/LPSE
prediction of $F_{hot}^{LPSE}(r,t)$

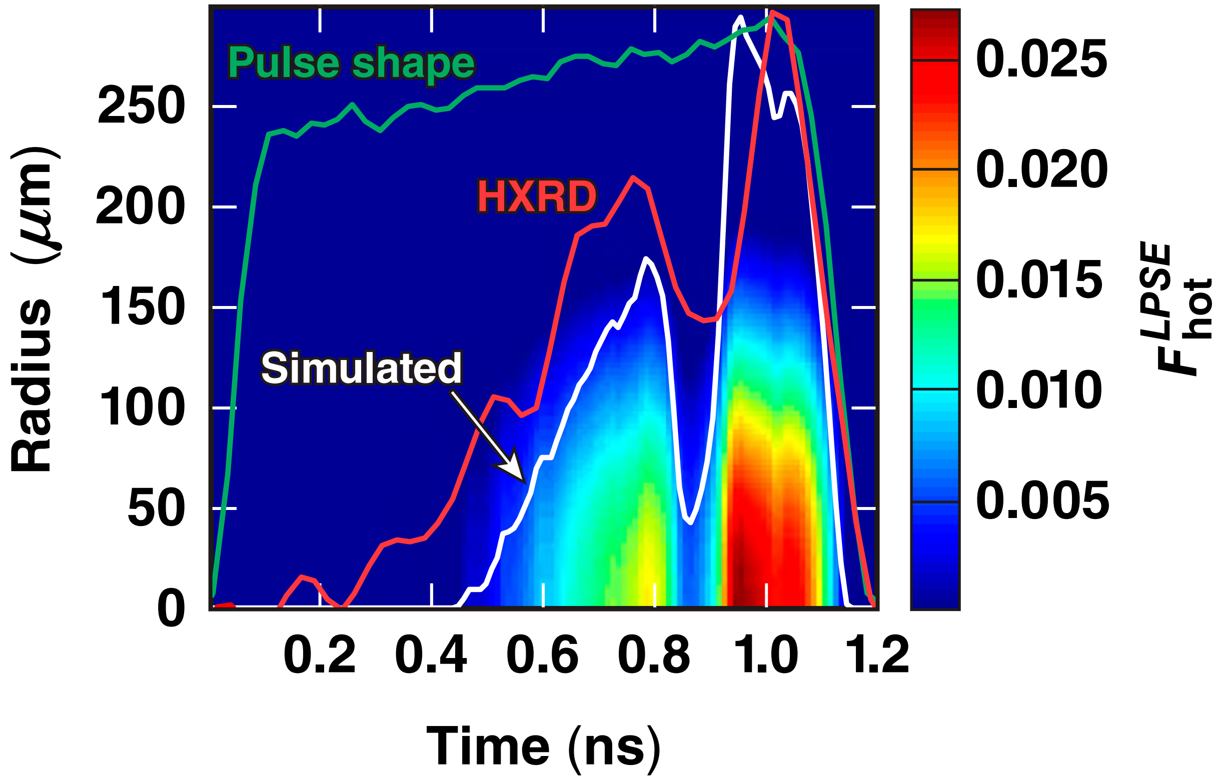

LPSE reproduces the observed scaling in hot-electron temperature and fraction

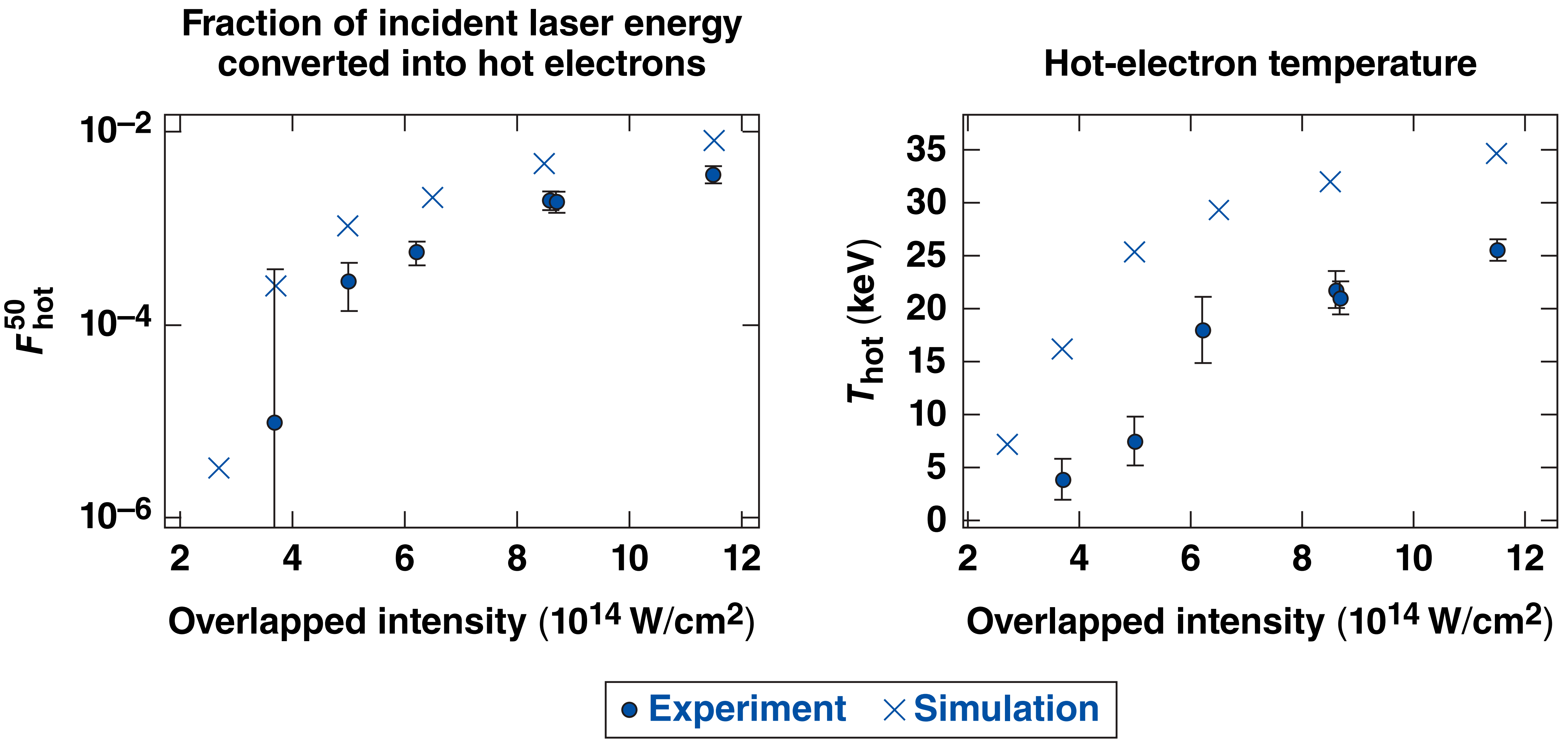

Three-dimensional two-plasmon–decay (TPD) simulations were used to reproduce experimental observations

- *LPSE* (laser-plasma simulation environment) was used to simulate Thomson-scattering (TS) from TPD-driven waves
- The Thomson-scattering spectra shows two large-amplitude peaks corresponding to TPD-driven waves
- A hybrid-particle model was used to calculate the hot-electron distribution
- The simulations reproduce the observed scaling of hot-electron temperature and fraction